Computers and Structures 275 (2023) 106937

Contents lists available at ScienceDirect

Computers and Structures

journal homepage: www.elsevier.com/locate/compstruc

Capacity controlled search: A new and efficient design-driven method for discrete size optimization of steel frames

Hasan Eser, Oğuzhan Hasançebi *

Middle East Technical University, Department of Civil Engineering, Ankara, Turkey

ARTICLE INFO

Article history:
Received 27 June 2022
Accepted 28 October 2022
Available online 11 November 2022

Keywords:
Structural optimization
Discrete sizing optimization
Steel frames
Design-driven search methods
Capacity controlled search algorithm

ABSTRACT

This paper presents a new and efficient design-driven method, called the capacity controlled search (CCS) algorithm, which is developed to handle sizing optimization of especially large-scale steel frames under multiple strength and displacement constraints. The CCS algorithm implements an intelligent and probabilistic search strategy, where the maximum demand-to-capacity ratios (DCRs) calculated for member groups are used to guide the search process for a rapid convergence to the optimum solution. The principle of virtual work or similar approaches that are commonly implemented by other design-driven methods are avoided in formulations of the CSS algorithm to make the method as simple and general as possible. The numerical performance of the proposed algorithm has been tested and verified on four steel frame design examples chosen from the literature. It is noted that the CCS algorithm produces the best-known solutions of these design examples in the literature until now. A statistical treatment of the independent runs performed with the CCS algorithm verifies robustness and reliability of the method.

1. Introduction

Structural optimization has long been studied in the literature using various methods. The early research in structural optimization field has been usually overwhelmed by the use of mathematical programming (MP) and optimality criteria (OC) methods [1]. Although these methods enable a considerably fast convergence to the optimum, they require gradient information to guide the search process, which in turn makes them impractical for handling discrete optimization problems. Moreover, the quality of the optimum solution (final design) obtained with these methods might be dependent on the starting point (initial design) of the optimization process such that the search usually converges to a local optimum nearest to the starting point. Hence, if the optimization process is initiated from a poor design point, it may end up in a poor local optimum, which may be far from the global one. Thus, some of these methods may fail to locate a global (or near-global) optimum, especially for complex design problems. Nevertheless, powerful gradient-based search methods are also available in the literature, such as such as sequential programming method (SQP), to find near-optimum solutions in the case of optimization problems with continuous variables.

In the last three decades, a group of non-traditional, stochastic, and derivative-free methods, which are commonly referred to as metaheuristic search methods, have emerged to be powerful tools and thus they have found abundance of applications in many disciplines of optimization, including the structural optimization [2]. These methods often come up with a promise of finding a good local optimum, if not the global one, even for complex problems. Besides, they can be applied to both discrete and continuous optimization problems. Typically, blind search strategies are employed by these methods, where the best solutions obtained so far are improved using random moves according to nature-inspired or swarm-intelligence based learning methodologies. Accordingly, these methods usually require a large number of function evaluations or response calculations, resulting in a slow convergence rate and usually a large amount of computing time. This even becomes more critical and significant for the optimization of large structural systems as the time needed to perform a vast number of finite element analyses in the course of optimization might be excessive, making the search process prohibitively impractical and inefficient.

In the literature, a time-efficient optimization of large structures with metaheuristic search techniques has been attempted in conjunction with several different approaches. One approach is

* Corresponding author.
E-mail addresses: heser@metu.edu.tr (H. Eser), oguzhan@metu.edu.tr (O. Hasançebi).

https://doi.org/10.1016/j.compstruc.2022.106937
0045-7949/

to establish a high-performance computing platform through a parallel or distributed computing. In this approach, the computational workload of the optimization algorithm is distributed to a cluster of interconnected processors for evaluating a population of designs concurrently [3–5]. However, apart from the fact that costly hardware set-ups are necessary in parallel/distributed computing, as compared to serial programming additional programming challenges arise, such as process synchronization, memory management, communication, deadlock, etc.

A second approach is to take advantage of surrogate models through the use of artificial neural networks or other similar response surface approximation methods, where force and/or deformation responses of a structural system are estimated, rather than implementing the exact and time-consuming finite element analyses [6–8] or constraint violations [9,10]. However, this requires a sufficiently large and diverse training set. The size of the training set might be too large and impractical for large-scale problems, yet the accuracy of approximation may not be guaranteed always.

In some studies in the literature, this problem has been addressed by developing hybrid optimization techniques, where two or more metaheuristic search algorithms are combined to produce an effective hybrid method that improves computational speed as well as quality of the optimum solution as compared to the cases where the techniques are implemented alone [11]. Although the number of structural analyses required cannot be drastically decreased via the hybrid optimization techniques, successful applications have been reported in structural optimization literature [12–18]. Recently, Kazemzadeh Azad [19] proposed several guided hybrid metaheuristic techniques where new candidate solutions were generated based on member demand-to-capacity ratios, resulting in significant computational savings in the early stages of optimization process in particular.

The aforementioned drawbacks of the metaheuristic search techniques have also led the researchers to develop new and alternative optimization methods which utilize analysis and design data to guide the search process for an accelerated convergence to the optimum solution. Such algorithms are commonly referred to as design-driven optimization techniques. Early examples of these techniques include the well-known fully stressed design (FSD) and its extensions: fully utilized design (FUD) and modified fully utilized design (MFUD) [20]. Although having a fast convergence rate, the fully stressed design method and its extensions may have some disadvantages. For example, FSD can only handle stress constraints. On the other hand, FUD can handle both stress and displacement constraints in a way such that the stress constraints are first calculated for all members of a structural system and then they are uniformly prorated by a factor determined based on the most violated displacement constraint. However, this usually leads to overdesign solutions because each member has a different contribution while controlling a particular displacement in a structure. MFUD provides improvements over FUD by using the Integrated Force Method (IFM), which identifies the critical members for each violated displacement constraint and, applies unequal prorating factors for different members.

One of the recent extensions of FSD is the Fully Stressed Design Evolution Strategy (FSD-ES) proposed by Ahrari and Atai [21]. The FSD-ES combines the design-driven deterministic approach of FSD with the global search capabilities of Evolution Strategy (ES). It has been shown that the method demonstrates superior performance in comparison to other techniques, producing the best results for some selected benchmark optimization problems in the literature. FSD-ES-II [22] provides further improvements over its predecessor by explicitly considering displacement constraints in the resizing step.

Another instance of the design-driven techniques is the fully constrained design (FCD) method proposed by Flager et al. [23]. This method utilizes the unit displacement method such that when a global displacement constraint is violated, the strain energy density (SED) corresponding to that particular displacement in the structure is calculated for each member. Both the strain energy densities and deflection scalars are normalized and multiplied with each other to calculate the constraint function for the global displacement. The optimization process is then guided based on the most critical constraint ratio of each design variable. It is important to note that the numerical applications of MFUD, FSD-ES, and FCD methods are limited to truss-type structures only.

Likewise, the principle of virtual work has been employed for structural optimization problems with displacement constraints in many other studies [24–29]. Among these studies, the guided stochastic search (GSS) method proposed by Kazemzadeh Azad et al. [28] and Kazemzadeh Azad and Hasançebi [29] is worth mentioning as it is directly applicable (no sectional transformation) to discrete sizing optimization of both frame and truss type structures under multiple displacement constraints. In this method, the principle of virtual work is utilized to determine the displacement participation factor (DPF) of each member for all displacement constraints separately. When normalized by the volume, this factor gives a sensitivity index (SI) that represents the effectiveness of a member in satisfying a displacement criterion. Later, the search process is guided based on the SI values and information gathered from previous analyses and design calculations.

This paper proposes a new design-driven optimization technique called capacity controlled search (CCS) for discrete size optimization of steel frames. The CCS method combines the coding simplicity of metaheuristic search algorithms with the computational efficiency of design-driven optimization approaches to achieve a rapid and reliable convergence to the optimum. Unlike the other design-driven optimization algorithms in the literature, the CCS method does not require utilization of the virtual work principle or other complex strategies to deal with displacement constraints. Besides, it produces a satisfactory optimum design by performing less than a thousand structural analyses even for the largest-scale structural optimization problems, for which hundreds of thousands of structural analyses or more are often required even by the most efficient metaheuristic search techniques.

The remaining sections of the paper are organized as follows. The second section presents a mathematical formulation for the optimum design problem of steel frames according to provisions of the AISC-LRFD [30] specification. The third section describes the working principle of the CCS method along with its detailed algorithm. In the fourth section, the numerical efficiency of the CCS method is investigated and quantified on the four selected steel frame examples, for which the optimum designs attained with the CCS method are compared with the previously published solutions to these problems in the literature in terms of the quality of optimum design and the number structural analyses performed. Finally, the last section highlights summary and important conclusions of the present study.

2. Problem formulation for discrete size optimization of steel frames

The size optimization of a steel frame can be defined as finding the minimum weight of the frame subject to strength and serviceability requirements imposed according to a chosen code of practice as well as geometric constraints between the members framing into each other at the same joints. It should be noted that in practical applications of steel frames, members must be selected from a set of commercially available steel sections only. Therefore,

a section pool that consists of a selected number of available steel sections is prepared prior to initialization of an optimization process. The steel sections are sorted in increasing order of a chosen sectional property; typically, the cross-sectional area. Each steel section in the pool is identified and referenced with a distinct sequence number that varies between 1 and the total number of sections in line with the sorted order of the sections in the pool. During the optimization process, selection and sizing of member groups are carried out in connection with the sequence numbers. That is to say, when a selection is made for a member group, cross-sectional properties for the selected section become available from the section pool through the sequence number.

For a steel frame consisting of N members collected in N_g member (sizing) groups, the optimization problem can be formulated as follows:

The objective is to find a vector of design variables $\mathbf{I}$, which minimizes the weight (W) of a structure subject to a number of design constraints (g_k).

$$\mathbf{I}^{\mathbf{T}} = [I_1, I_2, \cdots, I_{N_g}] \tag{1}$$

$$W = \sum_{i=1}^{N_g} \gamma_i A_i \sum_{j=1}^{N_m} L_j \tag{2}$$

$$g_k \le 0, k = 1, 2, \cdots, N_c \tag{3}$$

In Eqs. (1–3), the design variable vector $\mathbf{I}$ holds sequence numbers of the sections assigned to N_g member groups from the section pool; γ_i and A_i are the unit weight and area of the section assigned to a member group i, respectively; N_m is the total number of members in member group i; L_j is the length of the member j in member group i; g_k is the k-th normalized design constraint and N_c is the total number of design constraints.

The constraints of the optimization problem consist of various requirements imposed by design codes and construction practices. If the design process of a steel frame is performed according to the AISC-LRFD [30] specification, the following strength constraints must be satisfied for structural members:

(1) For members subjected to combined axial load and bending:

$$g_1 = \left(\frac{P_u}{\phi_a P_n}\right)_j + \frac{8}{9}\left(\frac{M_{ux}}{\phi_b M_{nx}} + \frac{M_{uy}}{\phi_b M_{ny}}\right)_j - 1.0 \le 0 \; for \left(\frac{P_u}{\phi_a P_n}\right)_j \ge 0.2 \tag{4}$$

$$g_1 = \left(\frac{P_u}{2\phi_a P_n}\right)_j + \left(\frac{M_{ux}}{\phi_b M_{nx}} + \frac{M_{uy}}{\phi_b M_{ny}}\right)_j - 1.0 \le 0 \; for \left(\frac{P_r}{\phi_a P_c}\right)_j < 0.2 \tag{5}$$

(2) For members subjected to shear:

$$g_2 = \left(\frac{V_u}{\phi_v V_n}\right)_j - 1 \le 0 \tag{6}$$

where P_u, M_u, and V_u are the required axial, flexural, and shear strengths calculated using the load combinations given in ASCE 7–98 [31], respectively; P_n, M_n, and V_n are the nominal axial, flexural, and shear strengths calculated according to the formulations given in the AISC-LRFD [30] specification; ϕ_a is the resistance factor for axial strength, which is 0.85 and 0.9 for compression and tension, respectively. The resistance factors for flexural strength (ϕ_b) and shear strength (ϕ_v) are both equal to 0.9; the subscripts x and y represent the strong and the weak axis of bending for member j.

In addition to the strength requirements, the following serviceability constraints are considered:

$$g_3 = \frac{\delta_i}{\delta_a} - 1 \le 0 \tag{7}$$

$$g_4 = \frac{\Delta_r}{\Delta_a} - 1 \le 0 \tag{8}$$

where δ_i and δ_a represent the calculated inter-story drift for i-th story in the frame and its allowable value, respectively. Similarly, Δ_r and Δ_a denote the maximum lateral displacement of the structure at the roof level and the corresponding allowable value, respectively.

From the practicality point of view, the following geometric constraints must be considered between beam and column members framing into each other at the same joints (Fig. 1):

(1) For beams connected to column flange:

$$g_5 = \frac{b_f^b}{b_f^c} - 1 \le 0 \tag{9}$$

(2) For beams connected to column web:

$$g_6 = \frac{b_f^b}{\left(h^c - 2t_f^c\right)} - 1 \le 0 \tag{10}$$

where h, b_f and t_f are the section depth, flange width, and flange thickness of a doubly symmetric steel section assigned to a member group, respectively; and the superscripts b and c denote the corresponding beam and column member groups, respectively.

The objective function given in Eq. (2) is only used for feasible designs. In case a infeasible design is generated, it is handled via external penalty function approach, where the total amount of constraint violation is added to the original objective function and its penalized objective function value is calculated using Eq. (11).

$$\phi = W[1 + Penalty(\mathbf{I})] = W\left[1 + r\left(\sum_{l=1}^{N_{LC}} \sum_{k=1}^{N_c} \max(0, g_k)\right)\right] \tag{11}$$

In Eq. (11), ϕ represents the penalized (constrained) objective function of a design vector $\mathbf{I}$; N_{LC} is the total number of design load combinations considered for the frame. The static penalty coefficient (r) is used to adjust the intensity of penalization as a whole. It is usually taken as 1.0.

A complete formulation of the optimum design problem is presented in Kazemzadeh Azad and Hasançebi [29], Kazemzadeh Azad

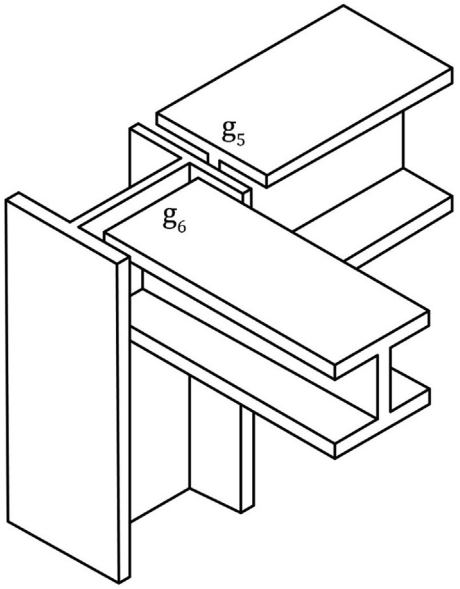

Fig. 1. Geometric constraints.

[32] and other former publications of the authors, including the detailed formulations for calculating nominal axial, bending and shear strengths of structural members according to the AISC-LRFD [30] specification.

3. Optimum design method

In this section, the capacity controlled search (CCS) technique is proposed and introduced for discrete sizing optimization of steel frame structures under multiple strength and displacement constraints. In the following subsections, the working mechanism behind this technique is explained first, and next its detailed algorithm is presented.

3.1. The working principle of CCS

The main idea behind the CCS technique lies in achieving effective utilization of structural components while resisting design loads. A structural component is locally subjected to strength constraints to ensure safety requirements. In addition, every structural component contributes -with varying levels- to satisfying a global displacement criterion, such as inter-story drift or roof drift.

In the absence of a global displacement criterion, a fully stressed design or in a broader sense, a fully utilized design, where each structural component is used at its utmost member strength and/or displacement capacity, generally results in cost-efficient designs. However, in practical design applications, there are often global displacement criteria that must be satisfied by an acceptable design.

The design-driven optimization techniques in the literature rely on the use of the unit load or the unit displacement method for determining structural elements that have a strong influence on controlling a global displacement criterion. Accordingly, when a global displacement criterion is violated, larger sections are assigned to those members initially in an effort to reduce the displacement quantities effectively. Although this strategy is certainly efficient for satisfaction of the violated displacement constraints rapidly, there is no guarantee that such a design guidance obtained from a displacement control strategy will lead the search towards the optimum design or even a good solution. Such design heuristics are avoided in the CCS method to maintain generality and simplicity of the optimization algorithm; instead, a probabilistic approach to retreat from an infeasible search direction is adopted.

3.2. Generation of a candidate design

In the CCS method, the current design is analyzed under all design load combinations, and the maximum demand-to-capacity ratio (DCR) for each member group is determined by considering strength constraints. A candidate design is then generated every time by selecting and perturbing a number of design variables in the current design. The selection of design variables is carried out probabilistically, yet in conjunction with the DCR values of member groups in the current design. In general, for member groups, very low values of DCR below one refer to overdesigned (ineffective) structural members, whereas very high values of DCR above one indicate underdesigned (insufficient) structural members. It follows that the section changes become more critical and necessary for these member groups to achieve a more efficient use of the material in terms of capacity utilization. Hence, in the CCS method the selection probability is set to minimum for member groups with DCR around one, and this probability increases proportionally as the DCR of a member group gets away from one.

The perturbations of selected design variables are also carried out based on some probabilistic rules. A member group with a DCR higher than 1.0 means that it fails to satisfy a design constraint and a larger section must be assigned. On the other hand, if its DCR is less than 1.0, a smaller section can be assigned to provide economy. At times when no global displacement constraint is imposed, ideally DCRs for all member groups should be adjusted to values around 1.0 to ensure the most effective use of the material in a structure. However, the presence of global displacement constraints might overwrite this rule to some extent because some global displacement quantities might be quite sensitive to the cross-sectional properties of some members, and the selection of larger sections for those members might be necessary to reduce the global displacements to the desired levels at the expense of having low DCR values for those particular members. Likewise, changing the sizes of some member groups in indeterminate structural systems may lead to overall force distributions such that not only the changed member groups but also the unchanged member groups are affected by this redistribution. For instance, for a member group with a DCR greater than unity, when the size of a different member group is changed, the member group in consideration (although not changed) may now be subjected to lesser loads, resulting in a DCR less than one. For these reasons, the CCS technique employs a simple probabilistic approach (via β parameter, which will be introduced in the next section) while deciding whether a larger or smaller section will be assigned to a member group. In this approach, a member group with a DCR value greater than 1.0 is given a greater chance to be assigned to a larger section; yet the possibility that the group might be assigned to a smaller section still exists but with a lesser probability. Conversely, a member group with a DCR value less than 1.0 is given a higher chance to pick a smaller section, but a larger section might also be assigned with a reduced possibility.

It is important to emphasize that the design process in the CCS method is ideally initiated by assigning the largest available section to each member group. Accordingly, at the beginning of the optimization process, most member groups are likely to have low DCR values. It follows that most of the design variables, if not all, are selected and modified in the early stages of the optimization process, leading to an effective explorative search of the design space. However, as the iterations continue and the better solutions are produced in the course of optimization, DCR values of the member groups will increase. Accordingly, a lesser number of design variables will be chosen and modified, implying that the exploitative capability of the algorithm will progressively be emphasized as the explorative capability reduces. While this provides a smooth and ideal transition from an explorative type search to exploitative one, member groups with DCR values close to one might constantly have very low selection probabilities and find no chance for section chance, impairing the search performance of the algorithm. This problem is overcome here by specifying a minimum selection probability (P_{min}, which will be introduced in the next section) for each member group.

3.3. Larger and smaller sections

The terms ‘‘larger” and ‘‘smaller” sections used in the CCS algorithm require particular attention and explanation. It is important to emphasize that in discrete structural optimization the sections that will be used to size member groups in a structure are sorted in ascending order of cross-sectional areas in a section pool (discrete set). Although the terms ‘‘larger” and ‘‘smaller” sections imply an increase and decrease in the cross-sectional area of a member group with respect to the existing section respectively, they may not always ensure increased or decreased sectional properties in favor of the member group. This is because in frame type structures multiple failure modes are usually available for structural members under the combined effect of axial force and bend-

ing moment. For example, one member may fail under shear; another member may fail under bending about the strong axis or weak axis, or local buckling mechanisms may be observed, etc. Hence, an increase in member size may also lead to the selection of a heavier yet weaker section; likewise, a decrease in member size might lead to the assignment of both lighter and stronger section to a member group.

In the early applications of structural optimization in the literature, structural analysis routines have been considered well-integrated and an inseparable part of structural optimization programs. However, with the advances in computer and software technologies, structural design and analysis programs (such as SAP2000) as well as finite element packages have started providing opportunities for application programming interface (API) type communication and interaction intermediaries, which in fact allow for these programs to be called and executed externally by other applications. If the design optimization process is performed in conjunction with an external structural analysis software, rather than using an integrated finite element routine, the limit states leading to the overcapacity of member groups may not always be made available by the software, or it may be uneasy to derive from the analysis results which mechanism actually caused the failure of a member group under consideration. One may think that a section having a larger cross-sectional area and moment of inertias about both bending axes than the existing one might be chosen to ensure the strongness of the former, which in turn eliminates the need for identifying the main failure mode. Alternatively, a correlation might be assumed between cross-sectional area and moment of inertias of the steel sections prior to the optimization process, and the sections which do not satisfy this correlation might be dismissed from selection to help accommodate a regular section pool [33]. Although both approaches guarantee the selection of a stronger section with an increase in member size, more economical sections that could have possibly provided the adequate strength required by the main failure mode will be omitted for sizing the member groups. Hence, neither of these strategies is implemented here. Instead, when an increase in member group size is required, one of the next larger sections in the section pool is assigned to the member group to enhance the explorative ability of the algorithm by sampling a large number of sections in a specified neighborhood. Similarly, when a decrease in member group size is promoted, one of the next smaller sections in a specified neighborhood in the section pool is assigned to the member group probabilistically to provide the algorithm an opportunity for sampling lighter yet stronger sections.

3.4. Stagnation control strategy

The CCS algorithm utilizes a basic stagnation control strategy based on uphill move to avoid entrapment at a local optimum. According to this strategy, if the best solution is not improved over a predetermined number of iterations, a stagnation escape period (SEP) is initiated by the algorithm. Before the SEP, the algorithm only allows for a design transition to better solutions; and hence the current design (also called elite design) represents the best solution obtained thus far in the optimization process. With the start of the SEP, the elitism rule is suspended temporarily, and a transition to a non-improving solution (uphill move) is allowed only for once provided that it has a penalized weight (constrained objective function value) not more than a predefined ratio (α) of the penalized weight of the elite design. Once the elite design is replaced by a non-improving design, the elitism rule is activated again within the SEP, and the following candidate designs are generated from this non-improving design, called temporary elite design. The temporary elite design is replaced and updated whenever a candidate solution better than the temporary elite design is generated within the SEP based on the elitism rule. On the other hand, if a candidate solution better than the elite design is produced, the SEP is terminated immediately and it becomes the elite design of the optimization process. If no improvement is achieved within the SEP, another SEP loop is initiated but this time uphill move is performed with reference to the last temporary elite design of the previous SEP.

3.5. Upper-bound strategy

The upper-bound strategy (UBS) proposed by Kazemzadeh Azad et al. [34] is utilized in the CCS algorithm to significantly reduce the number of structural analyses required during the optimization process. In fact, the principle of UBS lies in the idea of eliminating unnecessary structural analyses for candidate designs that have no chance to improve the current (elite) design. The UBS is very suitable for the CCS algorithm because the algorithm implements an elitism rule (except during SEP) for design transition, in which the current design is only replaced by an improving candidate solution. This strategy is implemented such that whenever a candidate solution is generated, the structural weight of the resulting design is calculated first. The structural analysis of the candidate design is implemented only if its structural weight is lower than the objective function (penalized weight, ϕ) of the elite design; otherwise, the candidate design is automatically eliminated without performing any structural analysis as it has no chance to improve the elite design anyway.

In the present study, the basic UBS approach is further improved such that not only the structural weight but also the constraints that do not require structural analysis for evaluation (e.g., geometric constraints) are considered together to calculate the penalized weight of a candidate design prior to the structural analysis, called pre-analysis objective function. A candidate design is analyzed only if its pre-analysis objective function is lower than the objective function of the elite design. This way even more candidate designs can be eliminated without performing structural analysis and substantial computational savings can be achieved. This version of the UBS proposed in this study is referred to as improved upper-bound strategy (iUBS).

3.6. The geometric constraint scaling factor

A high number of connections usually exist in large-scale structures, which might lead to extremely large and dominant geometric constraint violations in candidate designs generated in earlier stages of an optimization process. Accordingly, both feasible and improving candidate designs may not be generated easily, leading to a reduced search capability of the CCS algorithm at these stages. Hence, it is crucial that the dominance of geometric constraints is reduced to facilitate a thorough search process with the algorithm. This problem is tackled in the CCS algorithm by scaling down the effect of geometric constraint violations through multiplication with a scaling factor (Ω), which is dynamically adjusted throughout the optimization process, as follows:

$$\Omega_{iter} = \Omega_0^{\frac{iter^{max}-iter}{iter^{max}-1}} \tag{12}$$

where *iter* is the iteration number; $iter^{max}$ is the maximum number of iterations to be performed in the optimization process; and Ω_0 is the initial value of the scaling factor ($\Omega_0 < 1.0$), which is arbitrarily chosen small enough to allow for a generation of improving candidates that replace the current design. As the iteration number increases, Ω_{iter} will gradually approach to unity, making the effect of geometric constraints more pronounced.

3.7. The CCS algorithm

Given the principles and underlying ideas about the CCS method, its detailed algorithm can be presented as follows.

Step 1. Initiation: Prior to the optimization process, a section pool is prepared, where the steel sections that will be used to size member groups are collected and sorted in ascending order of their cross-sectional areas. The initial design is ideally formed by assigning the largest available sections to each member group. Then, this initial design is analyzed, and its penalized weight is calculated in accordance with Eq. (4). Besides, the maximum DCR is determined for each member group in the initial design by considering both strength and local displacement (e.g., deflection) constraints. The iteration number is set to one.

Step 2. Selection: A candidate design is then generated by selecting and perturbing a number of design variables in the current design. The selections of design variables are carried out probabilistically yet in conjunction with the DCR values of member groups using the following equations:

$$max\left(P_{min}, |1 - DCR_i|^{u}\right) \geq Rand_i \tag{13}$$

$$P_{min} = 1/N_g \tag{14}$$

In Eqs. (13) and (14), DCR_i is the maximum demand-to-capacity ratio for i-th member group (design variable); P_{min} is the minimum selection probability which is set to $1/N_g$; N_g is the total number of member groups; u is a parameter to adjust selection probability; and $Rand_i$ is a uniformly distributed random number between 0 and 1, which is sampled anew for each member group. If Eq. (13) is satisfied for a design variable, then it is selected for perturbation; otherwise, it is not selected.

Step 3. Perturbation: The perturbation of a selected design variable is conducted by stochastically assigning a new steel section within a search neighborhood. The width of a search neighborhood is defined first according to the adaptive search neighborhood width (nw_a) scheme, as follows:

$$nw_{a,i} = round\left(\sqrt{N_{sec,i} - 1}\right) \cdot \left(min(1, |1 - DCR_i|)^{\rho}\right) \tag{15}$$

$$nw_{min} \leq nw_{a,i} \tag{16}$$

In Eqs. (15) and (16), $N_{sec,i}$ is the number of available sections in the section pool associated with the member group i; ρ is a parameter used to adjust the rate of reduction in the search neighborhood width; and nw_{min} is the minimum search neighborhood width.

A new section within the search neighborhood ($nw_{a,i}$) is then assigned to the selected member group using the following equations:

$$I_i^{iter+1} = I_i^{iter} + round\left(\beta \cdot max\left(1, abs(Randn_i) \cdot nw_{a,i}\right)\right) \tag{17}$$

$$\beta = sign((DCR_i - 1) \cdot (\tau - Rand_i)) \tag{18}$$

where I_i^{iter} and I_i^{iter+1} are the sequence (index) numbers of the steel section assigned to the selected member group at iterations $iter$ and $iter + 1$, respectively; β is a probabilistic parameter that decides whether a larger or smaller section will be assigned to the selected member group; τ is a constant used to adjust β; $Randn_i$ is a normally distributed random number with zero mean and standard deviation of one; and $Rand_i$ is a uniformly distributed random number between 0 and 1. $Rand_i$ and $Randn_i$ are sampled anew for each member group.

Step 4. Analysis and Evaluation: The pre-analysis penalized weight (objective function) of the candidate design is calculated. If this value is higher than the objective function value of the elite design, the candidate is automatically rejected and the algorithm returns back to Step 2. Otherwise, a structural analysis is performed for the candidate design to obtain its force and deformation responses and to calculate its final penalized weight. If the candidate design has a lower penalized weight than that of the elite design, it replaces the current design and becomes the new elite design; otherwise, it is rejected.

Step 5. Stagnation Control: If the best solution is not improved over a predetermined number of iterations, SEP is initiated. If the algorithm is already in a SEP and if a candidate solution better than the elite design is produced at this stage, then the SEP is abandoned.

Step 6. Termination: The algorithm is terminated when a predefined stopping criterion is satisfied; such as reaching a predefined maximum number of iterations, $iter^{max}$ or failing to improve the elite design over a predefined number of iterations, $iter^{ni}$, etc. Otherwise, the iteration number is increased by one, and the steps 2–6 are repeated.

Flowchart of the design process via the CCS algorithm can be found in Fig. 2.

4. Design optimization examples

In this section, the performance of the CCS algorithm is investigated using four design examples chosen from the literature related to discrete sizing optimization of space steel frames. These examples are i) 135-member steel frame, ii) 1026-member steel frame, iii) 3860-member steel frame, and iv) 11540-member steel frame. It should be noted these design instances have been studied using relatively a large number of optimization algorithms in the literature; namely, UBS integrated Exponential/Modified Big-Bang Big Crunch (UEBB-BC/UMBB-BC) by Kazemzadeh Azad et al. [34,35]; Guided Stochastic Search (GSS) by Kazemzadeh Azad and Hasançebi [29]; Quantum-behaved Developed Swarm Optimizer (QDSO) by Talatahari and Azizi [36]; Tribe-Interior Search Algorithm (Tribe-ISA) by Talatahari and Azizi [37]; Migration-based Vibrating Particles System (VPS-MBLS) by Talatahari et al. [38]; Charged System Search (CSS) by Kaveh et al. [39]; Monitored Convergence Curve integrated EBB-BC/MBB-BC (MCC-EB/MCC-MB) by Kazemzadeh Azad [32] and Parallel Hybrid Slime Mould-Jaya Algorithm (PHSMJA) by Uğur [40].

The CCS optimization algorithm was coded in MATLAB R2019a, while structural analysis and design of structural models were carried out via SAP2000 v21.0.2 through an open application programming interface (OAPI). The optimization runs were performed on a PC with Intel i5-6500, 4-core, 3.2 GHz processor, and 16 GB DDR4 RAM operating at 2133 MHz frequency. The parameter set of the CCS algorithm employed in each design example is determined based on some preliminary runs and by considering the size and complexity of each design example (Table 1). It should be noted that since the CCS is a design-driven stochastic technique, fifteen independent runs have been performed in each design. The optimum designs (minimum weight designs) produced to these examples with the proposed CCS algorithm are compared with the formerly reported solutions to the problems by aforementioned metaheuristics and design-driven search techniques.

In these design examples, a single section pool consisting of 268 AISC standard wide-flange steel sections is used to size the member groups. The material properties of the steel are taken as follows: modulus of elasticity (E) = 200 GPa, yield strength (F_y) = 248.2 MPa, and unit density (ρ) = 7850 kg/m^3.

4.1. Design loads and load combinations

The following load combinations were considered for the designs of investigated steel frames in compliance with the ASCE 7–98 [31] specification:

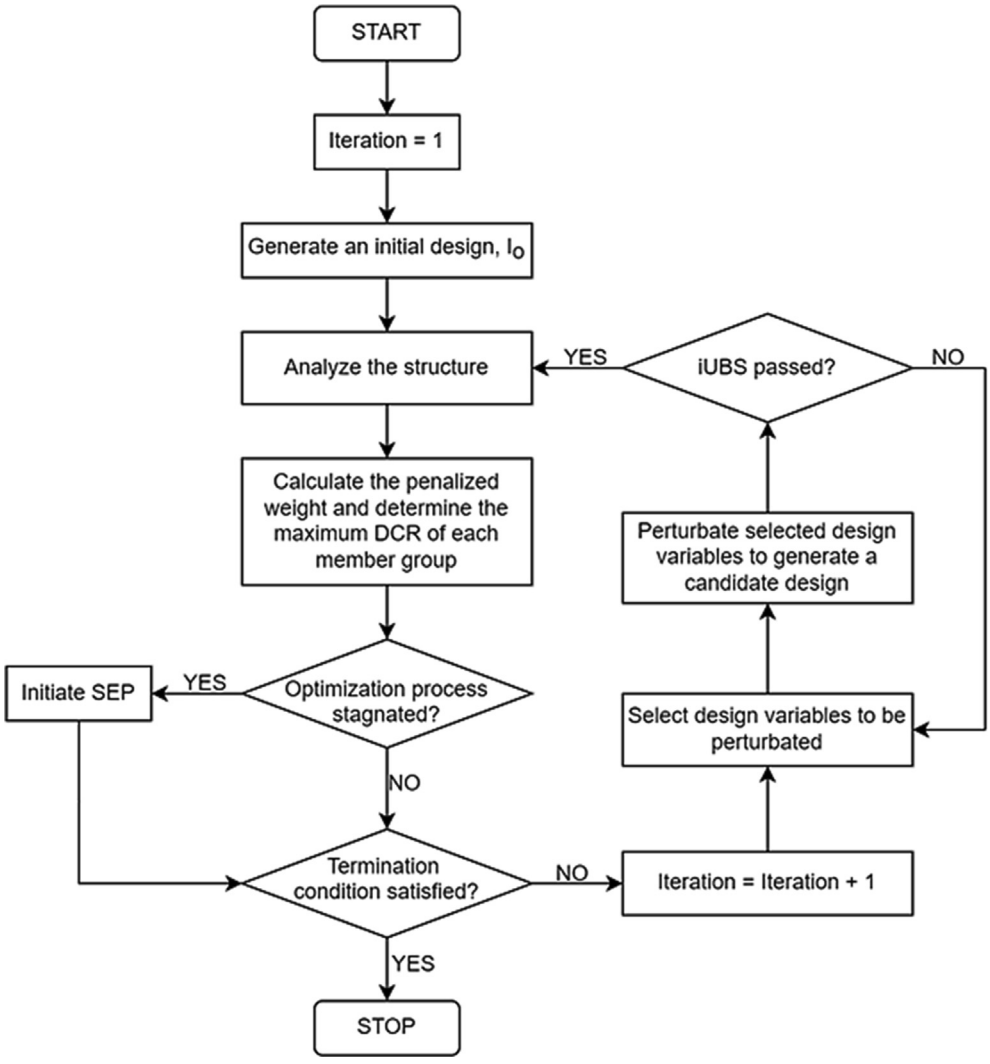

Fig. 2. Flowchart of the design process via the CCS algorithm.

Table 1
The parameter set of the CCS parameter employed in each design example.

	u	ρ	τ	α	SEP	$iter^{ni}$	$iter^{max}$	Ω_0
Example 1	2	3	0.8	1.1	25	100	500	1
Example 2	3	3	0.8	1.1	50	200	1000	0.0001
Example 3	2	3	0.8	1.1	50	200	1000	0.0001
Example 4	2	3	0.8	1.1	50	200	1000	0.0001

Table 2
Design loads, ELF procedure parameters, and displacement limits for the design examples.

	Dead Load (kN/m)		Live Load (kN/m)		Parameters for ELF			δ_a^{max}(m)	Δ_a^{max}(m)
	Floor Beams	Roof Beams	Floor Beams	Roof Beams	$T(sec)$	k	C_s		
Example 1	20	15	12	7	0.55	1.025	0.15	h/400	0.03
Example 2	20	15	12	7	1.267	1.380	0.10	h/400	0.10
Example 3	14	12	10	7	1.181	1.341	0.10	h/400	0.18
Example 4	15	12	12	7	1.181	1.341	0.10	h/400	0.18

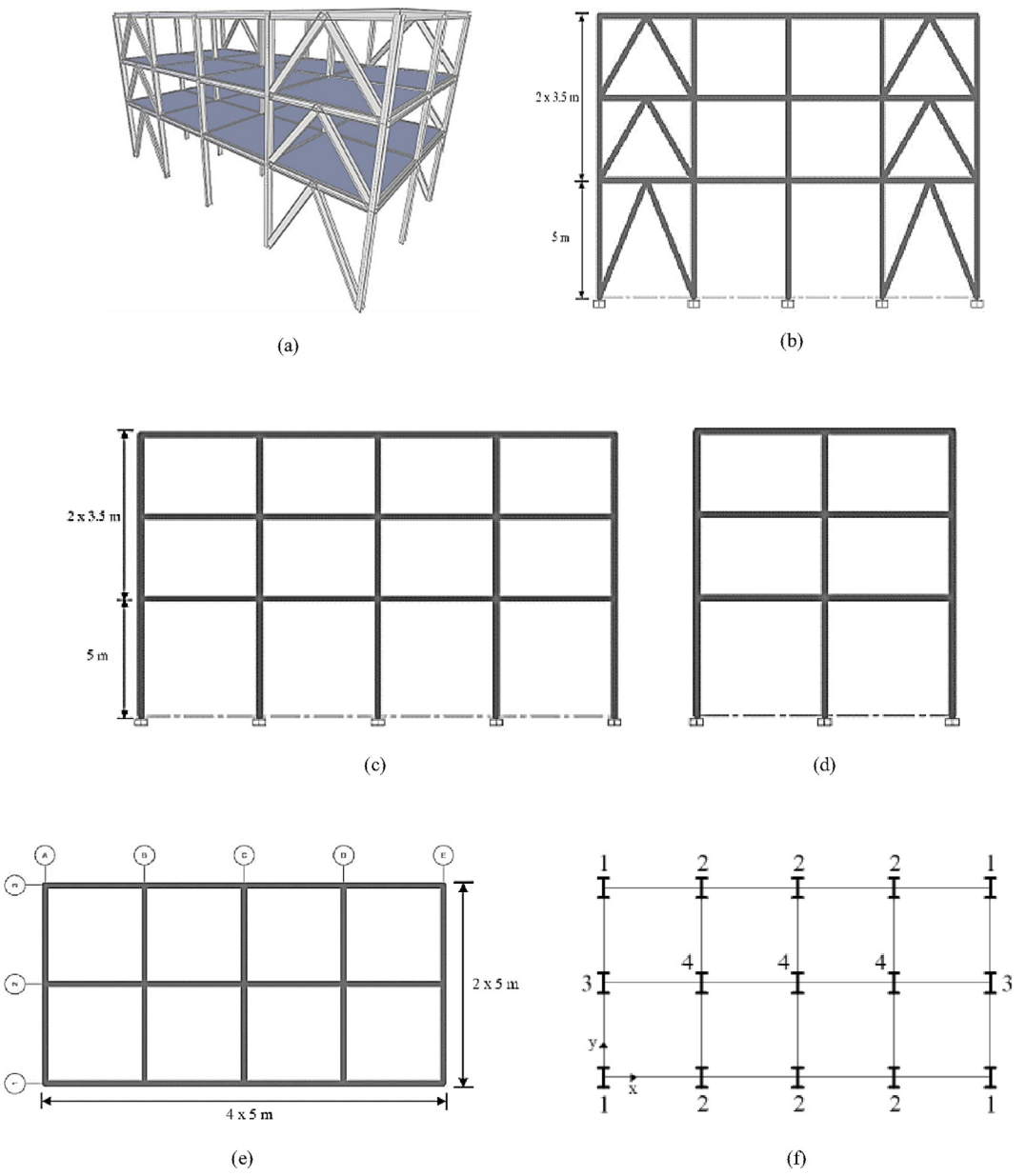

Fig. 3. 135-member steel frame: (a) 3-D view, (b) side view of the frames 1 and 3, (c) side view of the frame 2, (d) side view of the frames A to E, (e) plan view, and (f) grouping of the columns (Kazemzadeh Azad and Hasançebi, 2015).

Table 3
The optimum designs reported for the 135-member steel frame with various methods.

Group	GSS	MCC-EB	UEBB-BC	PHSMJA	CCS
CG_1	W16X36	W16X36	W21X62	W16X40	W14X48
CG_2	W18X60	W24X68	W14X48	W18X60	W21X62
CG_3	W12X40	W24X68	W36X150	W24X68	W18X60
CG_4	W30X108	W30X90	W21X68	W30X90	W24X76
B_1	W24X55	W16X26	W18X40	W18X35	W18X40
B_2	W18X35	W24X55	W18X35	W24X55	W21X44
B_3	W12X19	W12X16	W16X26	W12X16	W12X16
BR_1	W8X24	W8X24	W8X24	W8X24	W8X24
BR_2	W6X15	W14X22	W16X26	W6X15	W6X15
BR_3	W4X13	W4X13	W6X15	W4X13	W4X13
Best weight (ton)	37.12	36.76	38.91	36.97	35.81
Structural analyses	750	25,000	1235	22,064	396
Worst weight (ton)	47.92	38.42	–	41.67	39.88
Mean weight (ton)	42.12	37.33	–	39.90	37.56
Standard deviation	3.83	0.44	–	1.71	1.24
Coefficient of variation	0.09	0.01	–	0.04	0.03

Table 4
DCRs and maximum displacement constraint ratios in the reported optimum designs of the 135-member steel frame.

Group	GSS	MCC-EB	UEBB-BC	PHSMJA	CCS
CG_1	0.9931	1.0046	0.7183	0.9663	0.7491
CG_2	0.9963	0.8735	0.9187	0.9759	0.9969
CG_3	0.9407	0.8383	0.5980	0.8525	0.9471
CG_4	0.7662	0.8280	0.9008	0.8599	0.9604
B_1	0.6477	0.9262	0.7873	0.7926	0.7511
B_2	0.7411	0.5105	0.7488	0.4865	0.5958
B_3	0.8794	0.9853	0.6613	0.9843	0.9989
BR_1	0.9746	0.9196	0.9243	0.9310	0.9374
BR_2	0.7110	0.9777	0.8151	0.7156	0.7294
BR_3	0.8946	0.9166	0.5196	0.9317	0.9825
Max. DCR	0.9963	1.0046	0.9243	0.9843	0.9989
Min. DCR	0.6477	0.5105	0.5196	0.4865	0.5958
Mean DCR	0.8545	0.8780	0.7592	0.8496	0.8649
Standard deviation	0.1214	0.1350	0.1309	0.1464	0.1369
Max. IDR	0.9878	0.9478	0.9909	0.8903	0.9943
Max. Roof displacement	0.8846	0.8535	0.8503	0.8250	0.9553
Geometric constraints considered?	NO	NO	NO	YES	YES
Geometric constraints violated?	YES	YES	NO	YES	NO

1. 1.4D
2. 1.2D + 1.6L
3. 1.2D + 1.0E_x + 0.5L
4. 1.2D + 1.0E_{ex} + 0.5L
5. 1.2D + 1.0E_y + 0.5L
6. 1.2D + 1.0E_{ey} + 0.5L
7. 0.9D + 1.0E_x
8. 0.9D + 1.0E_{ex}
9. 0.9D + 1.0E_y
10. 0.9D + 1.0E_e

where D and L denote the dead and live loads, respectively; E_x and E_y are the earthquake loads applied at the center of mass in x and y directions, respectively; E_{ex} and E_{ey} are the earthquake loads applied considering the effect of accidental eccentricity of the center of mass in x and y directions, respectively. According to the ASCE 7–98 [31] specification, the amount of eccentricity is taken equal to 5 % of the dimension of the structure which is perpendicular to the direction of the applied earthquake load.

The gravity loads considered in each design example are given in Table 2. The earthquake loads were calculated and applied in accordance with the equivalent lateral force (ELF) procedure in the ASCE 7–98 [31] specification as follows:

$$F_x = \frac{w_x h_x^k V}{\sum_{i=1}^{n} w_i h_i^k} \tag{19}$$

where F_x is the design seismic load applied lateral seismic force at level x; w is the portion of the total gravity load assigned to the level i or x; h is the height from the base to the level i or x; and k is a parameter determined based on the period of the structure. It is equal to 1 for structures with a period less than or equal to 0.5 s, and equal to 2 for structures with a period of 2.5 s or more. For structures with a period between 0.5 and 2.5 s, k is determined by linear interpolation. The seismic base shear (V) in Eq. (19) is calculated as $V = C_s W$, where C_s is the seismic base shear coefficient and W is the total dead load of the building, which is subject to change during the optimization process. It should be emphasized that the period of the structure is calculated via the following equation in the ASCE 7–98 [31] specification:

$$T = C_T h_n^{3/4} \tag{20}$$

where h_n is the total height of the structure and C_T is the approximate period coefficient which is taken 0.0853 for the first and second examples, and 0.0488 for the third and fourth examples. For each design example, the values of T, k, C_s as well as the considered limits on the maximum inter-story drift (δ_a^{max}) and the maximum lateral displacement (Δ_a^{max}) are also provided in Table 2.

4.2. Design example 1: 135-member steel frame

The first design example is a 3-story and 135-member steel frame (Fig. 3) consisting of 45 columns, 66 beams, and 24 bracings. The stability of the frame is established using moment-resisting connections as well as inverted V-type bracing systems along the x-direction. The beam elements are continuously braced along their lengths by the floor system, while the columns and bracings are assumed to be unbraced along their lengths. The effective length factor, K, is taken as 1 for all the beams and bracings. The K factor is conservatively set to 1.0 for buckling of columns about their minor axis of bending since the frame is assumed to be non-swaying in that direction considering the inverted V-type bracing systems. On the other hand, the K factor for buckling of columns about their major axis of bending is determined using the respective formulations in the AISC-LRFD [30] specification. For practical fabrication requirements, the 135 members of the frame are grouped into 10 independent discrete sizing variables. The columns are collected under four different groups at the plan level as shown in Fig. 3f with no further grouping along the height of the frame. The beams in each story are grouped together, resulting in three beam groups. Similarly, the bracings in each story are grouped together, resulting in three bracing groups.

A comparison of the optimum design of the CCS technique with the previously reported solutions of this frame in the literature is presented in Table 3 in terms of the best design weight achieved and sectional designations attained for each member group. It can be seen from this table that the CCS outperforms all other methods in terms of both the quality of the optimum design and speed of convergence to the optimum solution. In fact, the CCS produces the best-known solution of this design example in the literature, resulting in an optimum design weight of 35.81 tons for the frame by implementing 396 structural analyses only. The solutions of the other methods are 37.12 tons obtained with 750 analyses by GSS; 36.76 tons obtained with 25,000 analyses by MCC-EB; 38.91 tons obtained with 1235 analyses by UEBB-BC, and 36.97 tons obtained with 22,064 analyses by PHSMJA. A statistical treatment of the fifteen independent runs performed with the CCS reveals

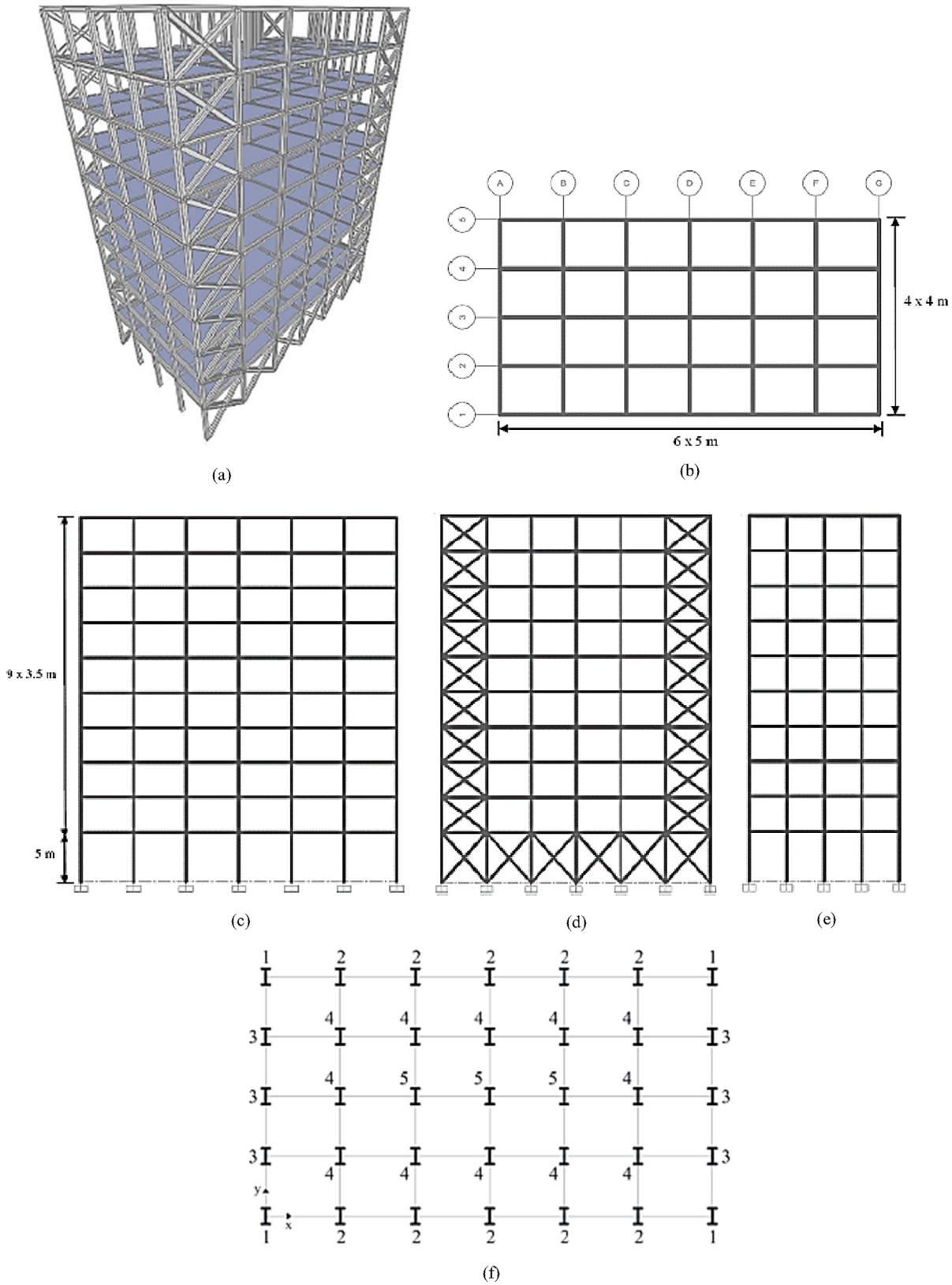

Fig. 4. 1026-member steel frame. (a) 3-D view, (b) plan view, (c) side view of the frames 2, 3 and 4, (d) side view of the frames 1 and 5, (e) side view of the frames A to G, (f) grouping of the columns (Kazemzadeh Azad, 2021).

Table 5
The optimum designs reported for the 1026-member steel frame with various methods.

Stories	Group	MCC-MB	UEBB-BC	ACSS	QDSO	Tribe-ISA	VPS-MBLSIII	PHSMJA	CCS
1	CG_1	W24X335	W33X201	W40X431	W36X359	W40X466	W36X245	W36X439	W44X230
	CG_2	W27X161	W24X146	W44X230	W36X182	W33X169	W24X117	W33X130	W36X194
	CG_3	W33X118	W24X104	W40X211	W33X221	W40X149	W24X176	W30X211	W30X116
	CG_4	W33X141	W40X174	W27X194	W36X182	W40X149	W40X174	W18X119	W36X160
	CG_5	W12X120	W40X321	W36X230	W33X221	W12X120	W21X132	W40X235	W40X183
	IB	W18X35	W27X84	W21X44	W14X26	W18X50	W8X18	W18X40	W12X22
	OB	W27X84	W27X84	W8X24	W18X46	W10X39	W33X152	W10X45	W24X55
	BR	W14X61	W18X76	W8X24	W10X54	W8X28	W8X31	W18X76	W10X68
2–4	CG_1	W36X328	W36X328	W12X230	W33X241	W40X297	W36X245	W33X291	W12X210
	CG_2	W36X170	W36X245	W30X235	W24X162	W24X146	W36X160	W30X173	W40X199
	CG_3	W33X118	W36X135	W33X241	W30X173	W27X94	W30X124	W36X182	W21X132
	CG_4	W36X135	W33X118	W30X116	W33X130	W24X117	W21X111	W30X99	W30X124
	CG_5	W30X108	W44X262	W21X132	W44X230	W24X117	W18X130	W30X173	W24X131
	IB	W21X44	W16X26	W14X22	W21X83	W24X76	W24X68	W16X31	W24X68
	OB	W27X84	W36X135	W33X118	W18X50	W16X50	W24X62	W33X118	W24X62
	BR	W24X68	W21X62	W10X49	W12X53	W14X68	W10X77	W10X54	W8X48
5–7	CG_1	W27X161	W27X258	W33X263	W14X159	W30X124	W40X167	W33X118	W30X116
	CG_2	W27X235	W18X106	W18X143	W33X201	W18X119	W14X145	W14X99	W30X173
	CG_3	W36X135	W33X130	W27X94	W40X149	W14X109	W30X116	W36X170	W33X141
	CG_4	W24X76	W27X94	W10X77	W14X74	W14X145	W16X77	W30X90	W12X87
	CG_5	W24X76	W24X192	W24X103	W21X93	W27X178	W16X100	W24X131	W14X68
	IB	W21X44	W21X44	W21X44	W16X31	W30X99	W18X40	W21X44	W16X26
	OB	W30X90	W21X73	W33X130	W33X118	W16X36	W33X130	W30X90	W30X99
	BR	W12X40	W30X90	W12X53	W10X45	W8X40	W18X60	W12X58	W12X50
8–10	CG_1	W30X90	W18X86	W18X86	W18X97	W12X96	W27X102	W30X173	W12X53
	CG_2	W24X104	W21X50	W14X74	W12X53	W14X176	W14X109	W14X132	W14X132
	CG_3	W24X76	W36X135	W18X76	W36X160	W27X84	W24X94	W27X84	W30X90
	CG_4	W30X90	W33X201	W21X93	W8X35	W16X77	W33X141	W14X109	W14X48
	CG_5	W24X104	W30X108	W12X170	W14X132	W33X130	W16X45	W10X45	W12X53
	IB	W16X31	W21X57	W14X30	W16X31	W16X26	W21X50	W16X26	W21X44
	OB	W16X26	W16X26	W21X62	W24X62	W18X55	W12X30	W21X44	W24X68
	BR	W12X58	W18X76	W16X77	W14X68	W18X55	W12X65	W14X34	W8X35
Best weight (ton)		504.34	584.93	540.38	530.33	532.44	534.11	508.43	500.68
Structural analyses		50,000	724	21,000	16,000	16,000	11,000	37,278	969
Worst weight (ton)		597.99	–	–	–	–	556.05	562.75	557.73
Mean weight (ton)		537.33	–	581.75	–	579.36	543.65	533.51	529.61
Standard deviation		27.77	–	21.75	–	22.26	6.57	20.46	12.91
Coeff. of variation		0.05	–	0.04	–	0.04	0.01	0.04	0.02

that the algorithm produces a mean design weight of 37.56 tons with a standard deviation of 1.24 and a coefficient of variation of 0.03, indicating its robustness and reliability.

The feasibility of the optimum designs produced to this design example by the CCS algorithm and other methods is investigated in Table 4 by presenting the maximum demand-to-capacity ratios (DCR) for each member group, the maximum inter-story drift ratio (IDR), and the maximum roof displacement in each solution reported. It can be seen from this table that the solutions reported by all the methods satisfy all the strength and displacement requirements outlined in Section 2, except MCC-EB. It is observed that the maximum DCR is slightly violated for the first column group (CG_1) in the solution reported with MCC-EB method.

The last two rows of Table 4 indicate whether the geometric constraints have been considered while solving the problem by different methods, and any geometric constraint violation is detected in the reported optimum solutions. It is important to emphasize that the consideration of geometric constraints not only restricts the feasible design space to a large extent but also hampers the search process in those restricted regions, making the problem more challenging and complicated for optimization algorithms. It is noted that the geometric constraints are not considered and imposed while solving the problem with GSS, MCC-EB, and UEBB-BC methods. Hence, those constraints, as anticipated, are not satisfied in the reported optimum solutions of the problem with the GSS and MCC-EB methods, yet they are inherently satisfied in the solution of the UEBB-BC method. On the other hand, a design check and verification process performed by the authors indicate that the optimum solution of the problem reported with the PHSMJA method slightly violates geometric constraints in the order of 0.57 %, and no such constraint violations are identified in the optimum solution obtained with the CCS algorithm in this study.

4.3. Design example 2: 1026-member steel frame

The second design example is a 10-story and 1026-member steel frame (Fig. 4) consisting of 350 columns, 580 beams, and 96 bracings. The stability of the frame is established using moment-resisting connections as well as X-type bracing systems along the *x*-direction. For all beam elements the unbraced lengths are set to one-fifth of their lengths, while the columns and bracings are assumed to be unbraced along their lengths. The effective length factor, *K*, is taken as 1 for all the beams and bracings. The *K* factor is conservatively set to 1.0 for buckling of columns about their minor axis of bending since the frame is assumed to be non-swaying in that direction considering the X-type bracing systems. On the other hand, the *K* factor for buckling of columns about their major axis of bending is determined using the respective formulations in the AISC-LRFD [30] specification. For practical fabrication requirements, the 1026 members of the frame are grouped into 32 independent discrete sizing variables. The member grouping is performed both at the plan and elevation levels. At the plan level, the columns are collected under five different groups (CG_1 to CG_5) as shown in Fig. 4f; the beams are collected under two groups as inner and outer beams; and all the bracings are assigned to a single

Table 6
DCRs and maximum displacement constraint ratios in the reported optimum designs of the 1026-member steel frame.

Stories	Group	MCC-MB	UEBB-BC	ACSS	QDSO	Tribe-ISA	VPS-MBLSIII	PHSMJA	CCS
1	CG_1	0.6635	0.8221	0.5260	0.5663	0.5636	0.8615	0.6210	0.7836
	CG_2	0.7481	0.7692	0.6346	0.7525	0.9177	1.0387	0.9016	0.7643
	CG_3	0.9929	0.8005	0.5653	0.5953	0.7826	0.7231	0.5758	0.9973
	CG_4	0.9972	0.7466	0.6077	0.7385	1.0073	0.7629	0.9959	0.8476
	CG_5	0.9240	0.5631	0.6093	0.6455	0.9589	0.9108	0.8237	0.8152
	IB	0.8155	0.5631	0.6646	0.7526	0.7083	1.4928	0.7786	0.9092
	OB	0.8606	0.5551	1.0754	0.7090	0.6081	0.6175	0.6123	0.8010
	BR	0.9067	0.8121	2.5951	0.8425	2.5649	1.8758	0.7833	0.7624
2–4	CG_1	0.5497	0.5083	0.7099	0.7499	0.7858	0.6716	0.5986	0.7761
	CG_2	0.8746	0.7955	0.9437	0.8276	0.7957	0.8448	0.7945	0.7982
	CG_3	0.9553	0.9538	0.5773	0.5536	0.9317	1.0902	0.7685	0.7878
	CG_4	0.7580	0.8536	0.8933	0.7465	0.9189	0.8488	1.0127	0.8416
	CG_5	0.9323	0.4744	0.7963	0.5432	0.8622	0.7706	0.6640	0.7623
	IB	0.8643	0.8291	0.8942	0.7326	0.8134	0.7566	0.8330	0.8176
	OB	0.9214	0.7608	0.8605	0.7326	0.7799	0.8066	0.8429	0.8308
	BR	0.8257	0.8463	0.7710	0.7156	0.6247	0.5568	0.6961	0.9429
5–7	CG_1	0.5757	0.3873	0.4238	0.6718	0.7298	0.6433	0.7125	0.7962
	CG_2	0.6214	0.7888	0.7760	0.7314	0.7208	0.8146	0.9538	0.7457
	CG_3	0.7299	0.8830	1.0701	0.7566	0.6703	0.9078	0.6793	0.7406
	CG_4	0.9682	0.7231	0.8783	0.8616	0.7243	0.8895	0.7862	0.7487
	CG_5	0.9161	0.4742	0.7797	0.9416	0.5712	0.7134	0.6147	0.9631
	IB	0.9039	0.8981	0.7877	0.8366	0.5527	0.7497	0.7995	0.8754
	OB	0.7664	0.8011	0.6360	0.6355	0.8482	0.6158	0.7013	0.7928
	BR	0.9881	0.5094	0.5653	0.8592	0.9240	0.9630	0.6423	0.8510
8–10	CG_1	0.4541	0.4925	0.4851	0.4903	0.4961	0.4264	0.3098	0.6170
	CG_2	0.5459	0.9711	0.6605	0.8540	0.4047	0.6162	0.6556	0.6102
	CG_3	0.6967	0.4185	0.8763	0.5501	0.5598	0.6155	0.7632	0.8020
	CG_4	0.5997	0.3545	0.6007	1.0076	0.6750	0.4005	0.4656	0.8394
	CG_5	0.3859	0.6094	0.2745	0.3398	0.3754	0.8863	0.8348	0.6885
	IB	0.9961	0.6711	0.8732	0.8293	0.9251	0.7679	1.0616	0.7362
	OB	0.9088	0.8482	0.5540	0.6940	0.7422	0.8851	0.7643	0.6127
	BR	0.3539	0.3044	0.3383	0.3391	0.6404	0.2809	0.8862	0.5922
Max. DCR		0.9972	0.9711	2.5951	1.0076	2.5649	1.8758	1.0616	0.9973
Min. DCR		0.3539	0.3044	0.2745	0.3391	0.3754	0.2809	0.3098	0.5922
Mean DCR		0.7813	0.6809	0.7595	0.7063	0.7870	0.8064	0.7479	0.7891
Standard deviation		0.1837	0.1852	0.3799	0.1507	0.3567	0.2896	0.1549	0.0949
Max. IDR		0.9948	0.9705	0.9948	0.9745	0.9800	0.9628	0.9782	0.9999
Max. Roof disp.		0.7754	0.6748	0.7755	0.7174	0.7538	0.7200	0.7357	0.7557
Geometric constraints considered?		NO	NO	NO	NO	NO	NO	YES	YES
Geometric constraints violated?		NO	YES	YES	NO	NO	YES	NO	NO

group. At the elevation level, the structural members are required to have the same sections in every three stories, except the first one, resulting in 20 column groups, 8 beam groups, and 4 bracing groups for the frame.

A comparison of the optimum design of the CCS technique with the previously reported solutions of this frame in the literature is presented in Table 5. It can be seen from this table that the CCS outperforms all other methods in terms of the quality of the optimum design achieved, and it ranks second in terms of speed of convergence to the optimum solution. In fact, the CCS produces the best-known solution of this design example in the literature, resulting in an optimum design weight of 500.68 tons for the frame by implementing 969 structural analyses only. The solutions of the other methods are 504.34 tons obtained with 50,000 analyses by MCC-MB; 584.93 tons obtained with 724 analyses by UEBB-BC; 540.38 tons obtained with 21,000 analyses by ACSS; 530.33 tons obtained with 16,000 analyses by QDSO; 532.44 tons obtained with 16,000 analyses by Tribe-ISA; 534.11 tons obtained with 11,000 analyses by VPS-MBLSIII; and 508.43 tons obtained with 37,278 analyses by PHSMJA. A statistical treatment of the fifteen independent runs performed with the CCS reveals that the algorithm produces a mean design weight of 529.61 tons with a standard deviation of 12.91 and a coefficient of variation of 0.02, indicating its robustness and reliability.

In Table 6, the feasibility of the optimum designs produced to this design example by the CCS algorithm and other methods is investigated in terms of related strength and displacement constraints. It can be seen from this table that amongst the reported solutions of the problem, those produced by the MCC-MB, UEBB-BC, and CCS methods satisfactorily meet all of the strength and displacement requirements, whereas those produced by ACSS, QDSO, Tribe-ISA, and VPS-MBLSIII method fail to satisfy strength requirements at least for one design group. It is also important to note that as compared to the other feasible solutions of the problem, the CCS algorithm yields an optimum design having the highest mean (0.7891) and the lowest standard deviation (0.0949) for DCR values of the member groups, indicating that a more uniform and efficient overall strength demand distribution is achieved for the frame with the proposed CCS algorithm.

Table 6 also analyzes whether the geometric constraints have been considered while solving the problem by different methods, and whether any geometric constraint violation is detected in the reported optimum solutions. It is noted that the geometric constraints are not considered and imposed while solving the problem with MCC-MB, UEBB-BC, ACSS, QDSO, and Tribe-ISA methods. Nevertheless, the reported optimum solution of the problem with the MCC-MBB satisfies those constraints inherently. Similarly, the geometric constraints are also inherently satisfied in the optimum

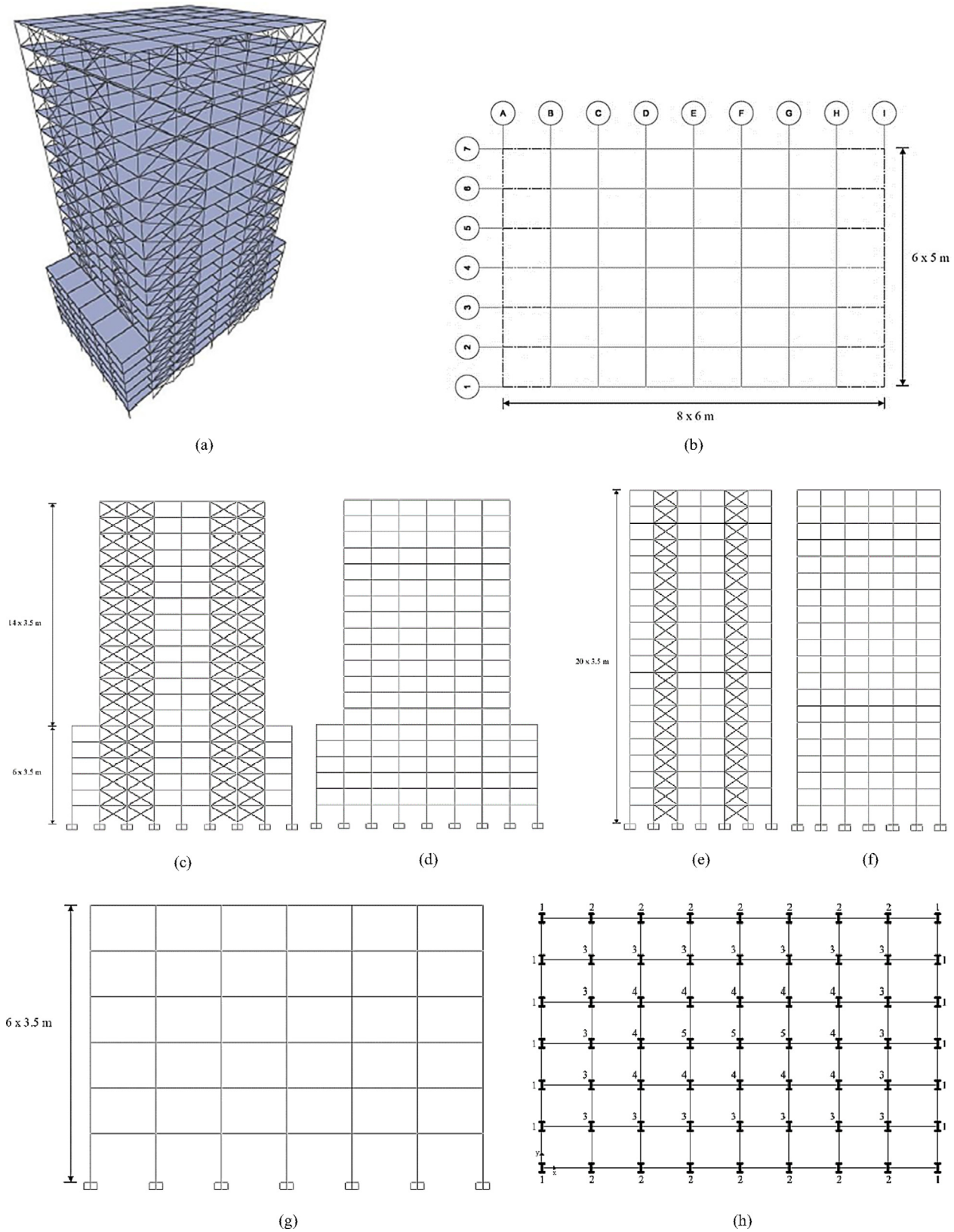

Fig. 5. 3860-member steel frame. (a) 3-D view, (b) plan view, (c) side view of the frames 1, 3, 5 and 7, (d) side view of the frames 2, 4, and 6, (e) side view of the frames B, D, F and H, (f) side view of the frames C, E and G, (g) side view of the frames A & I, (h) orientation and grouping of the columns (Kazemzadeh Azad and Hasançebi, 2015).

Table 7
The optimum designs reported for the 3860-member steel frame with various methods.

Stories	Groups	GSS	MCC-EB	UEBB-BC	QDSO	VPS-MBLSIII	PHSMJA	CCS
1–2	CG_1	W24X94	W40X235	W27X146	W12X79	W24X131	W40X167	W18X86
	CG_2	W27X368	W44X262	W12X210	W27X217	W14X145	W44X290	W40X297
	CG_3	W30X477	W36X328	W36X359	W40X392	W24X335	W44X290	W24X335
	CG_4	W40X199	W40X278	W40X593	W18X311	W14X500	W40X249	W12X305
	CG_5	W30X191	W36X527	W8X67	W36X135	W21X132	W44X290	W40X211
	IB	W12X152	W16X26	W40X183	W24X76	W12X79	W30X90	W12X26
	OB	W10X30	W30X99	W14X22	W16X100	W24X84	W33X130	W12X22
	BR	W14X82	W27X84	W40X167	W10X45	W12X65	W30X90	W18X86
3–4	CG_1	W18X65	W36X170	W40X167	W12X40	W12X53	W36X194	W12X53
	CG_2	W36X439	W40X215	W12X230	W40X331	W33X169	W40X278	W30X235
	CG_3	W44X335	W36X230	W36X650	W21X201	W24X492	W44X230	W24X250
	CG_4	W36X170	W33X201	W24X335	W14X370	W36X260	W40X183	W40X235
	CG_5	W30X191	W40X466	W14X68	W14X132	W14X132	W36X232	W27X194
	IB	W14X176	W12X30	W16X26	W21X68	W14X48	W24X84	W24X55
	OB	W12X40	W14X74	W40X235	W21X62	W14X48	W33X141	W10X26
	BR	W18X119	W40X149	W12X53	W10X54	W10X88	W30X90	W16X67
5–6	CG_1	W18X71	W44X262	W24X335	W12X26	W14X48	W40X149	W16X50
	CG_2	W44X335	W36X194	W27X178	W21X111	W10X112	W40X249	W33X201
	CG_3	W40X297	W44X230	W27X539	W24X335	W40X235	W33X221	W27X217
	CG_4	W36X160	W44X290	W36X439	W12X305	W30X326	W40X183	W24X207
	CG_5	W27X161	W36X245	W30X99	W30X261	W14X90	W36X210	W21X182
	IB	W18X71	W24X62	W44X230	W30X90	W18X71	W30X90	W21X73
	OB	W27X114	W16X40	W14X26	W12X53	W14X68	W33X141	W12X26
	BR	W33X152	W24X84	W12X72	W14X53	W10X112	W24X84	W10X60
7–8	CG_1	N.A.	N.A.	N.A.	N.A.	N.A.	N.A.	N.A.
	CG_2	W40X235	W44X230	W27X368	W36X135	W12X96	W36X194	W33X221
	CG_3	W24X207	W33X241	W18X234	W40X235	W40X278	W40X249	W27X217
	CG_4	W14X159	W36X256	W33X221	W40X372	W14X159	W36X150	W40X215
	CG_5	W12X210	W44X335	W40X321	W18X130	W21X132	W40X249	W27X161
	IB	W30X99	W40X183	W12X72	W12X72	W18X76	W40X149	W27X84
	OB	W8X35	W36X210	W33X130	W24X103	W24X250	W36X150	W30X90
	BR	W12X53	W21X83	W12X72	W21X73	W14X68	W12X65	W8X58
9–10	CG_1	N.A.	N.A.	N.A.	N.A.	N.A.	N.A.	N.A.
	CG_2	W36X194	W44X262	W30X326	W12X106	W33X169	W36X160	W36X182
	CG_3	W24X250	W36X160	W14X455	W27X161	W24X279	W44X230	W40X149
	CG_4	W40X183	W40X183	W12X120	W33X263	W24X408	W44X230	W21X201
	CG_5	W21X147	W18X143	W18X86	W10X88	W27X194	W40X149	W40X149
	IB	W40X211	W24X62	W27X94	W18X106	W33X118	W30X90	W27X94
	OB	W30X124	W33X130	W44X230	W27X84	W12X72	W33X118	W18X40
	BR	W18X76	W33X118	W24X84	W14X53	W8X40	W12X65	W8X67
11–12	CG_1	N.A.	N.A.	N.A.	N.A.	N.A.	N.A.	N.A.
	CG_2	W21X182	W36X160	W30X99	W18X119	W27X84	W40X149	W36X280
	CG_3	W12X210	W24X176	W12X305	W24X192	W36X160	W40X149	W30X235
	CG_4	W24X192	W44X335	W30X261	W36X256	W18X130	W44X230	W14X193
	CG_5	W24X162	W40X183	W44X230	W14X82	W16X89	W40X167	W12X136
	IB	W40X149	W30X90	W44X230	W30X90	W33X141	W24X55	W27X84
	OB	W10X54	W33X118	W40X149	W21X73	W18X97	W40X149	W36X150
	BR	W16X67	W30X90	W16X77	W10X19	W14X74	W10X60	W12X45
13–14	CG_1	N.A.	N.A.	N.A.	N.A.	N.A.	N.A.	N.A.
	CG_2	W14X159	W14X132	W16X89	W14X370	W14X61	W44X230	W27X161
	CG_3	W40X264	W40X149	W40X174	W30X173	W12X72	W40X174	W40X149
	CG_4	W27X102	W33X118	W16X100	W36X260	W44X262	W44X230	W14X145
	CG_5	W27X129	W36X260	W10X100	W14X99	W16X89	W44X230	W14X109
	IB	W10X77	W18X35	W14X43	W14X90	W21X68	W30X90	W21X68
	OB	W33X318	W30X99	W36X135	W18X130	W10X54	W36X150	W24X68
	BR	W16X67	W21X62	W33X152	W10X17	W8X40	W10X60	W12X50
15–16	CG_1	N.A.	N.A.	N.A.	N.A.	N.A.	N.A.	N.A.
	CG_2	W18X86	W33X118	W12X79	W30X132	W36X170	W44X230	W30X99
	CG_3	W36X232	W14X82	W44X262	W36X170	W12X136	W14X99	W33X141
	CG_4	W14X90	W12X87	W24X250	W33X118	W40X183	W14X99	W36X160
	CG_5	W12X79	W24X279	W33X263	W12X87	W24X103	W14X99	W24X117
	IB	W27X129	W12X26	W30X132	W21X73	W18X60	W14X53	W30X99
	OB	W10X26	W14X26	W14X68	W33X201	W12X79	W24X62	W14X26
	BR	W21X83	W24X68	W21X62	W10X19	W8X31	W10X60	W8X40
17–18	CG_1	N.A.	N.A.	N.A.	N.A.	N.A.	N.A.	N.A.
	CG_2	W21X83	W14X74	W24X117	W14X53	W10X49	W36X135	W16X77
	CG_3	W18X119	W40X199	W40X167	W8X58	W27X194	W14X68	W24X76
	CG_4	W16X67	W27X102	W36X245	W27X84	W36X150	W14X48	W30X90
	CG_5	W18X65	W33X169	W30X292	W18X65	W27X146	W14X99	W21X62
	IB	W18X35	W21X44	W40X149	W24X68	W16X67	W14X48	W14X26
	OB	W18X35	W40X174	W33X141	W10X88	W18X86	W24X62	W24X55
	BR	W10X45	W18X50	W14X48	W18X55	W8X31	W10X60	W18X50

Table 7 (*continued*)

Stories	Groups	GSS	MCC-EB	UEBB-BC	QDSO	VPS-MBLSIII	PHSMJA	CCS
19–20	CG_1	N.A.	N.A.	N.A.	N.A.	N.A.	N.A.	N.A.
	CG_2	W10X30	W30X108	W36X300	W12X65	W16X57	W14X99	W18X55
	CG_3	W10X33	W14X48	W18X60	W10X68	W27X114	W30X108	W18X55
	CG_4	W36X210	W16X77	W44X230	W40X264	W12X120	W12X65	W12X30
	CG_5	W10X100	W40X277	W10X54	W24X146	W18X119	W14X99	W12X30
	IB	W36X150	W16X36	W21X50	W18X86	W12X53	W14X53	W14X22
	OB	W16X45	W40X174	W30X116	W10X60	W21X93	W24X62	W16X31
	BR	W16X45	W12X65	W24X62	W10X17	W8X24	W8X28	W8X28
Best weight (ton)		3539.83	2972.64	4117.43	2703.32	2787.50	3013.10	2353.65
Structural analyses		900	50,000	9979	17,000	20,000	48,622	997
Worst weight (ton)		4069.65	3494.69	–	–	3066.63	3510.50	2633.76
Mean weight (ton)		3776.41	3245.55	–	–	2927.05	3229.10	2446.31
Standard deviation		183.36	138.45	–	–	97.22	220.00	78.89
Coeff. of variation		0.05	0.04	–	–	0.03	0.07	0.03

Table 8
DCRs and maximum displacement constraint ratios in the reported optimum designs of the 3860-member steel frame.

Stories	Groups	GSS	MCC-EB	UEBB-BC	QDSO	VPS-MBLSIII	PHSMJA	CCS
1–2	CG_1	0.6811	0.3479	0.4980	0.6196	0.5773	0.5322	0.6972
	CG_2	0.8026	0.9794	0.8684	1.1193	1.2949	0.9010	0.8917
	CG_3	0.8284	0.9673	0.8230	0.9654	1.2011	0.8897	0.9972
	CG_4	0.9642	0.9141	0.5159	0.9708	0.6564	0.8299	0.8155
	CG_5	0.8816	0.4493	0.9959	1.2238	1.0382	0.7058	0.8914
	IB	0.3430	0.6522	0.4290	0.5838	0.4779	0.4160	0.8103
	OB	0.8365	0.4539	0.8334	0.2535	0.4098	0.3094	0.9931
	BR	0.7095	0.8464	0.4702	1.4097	0.7241	0.7743	0.7651
3–4	CG_1	0.7500	0.3573	0.7113	0.9926	0.7859	0.4650	0.8194
	CG_2	0.5188	0.9531	0.8000	0.6587	0.9912	0.8874	0.8894
	CG_3	0.7758	0.8916	0.4765	1.2130	0.5855	0.9639	0.9069
	CG_4	0.8662	0.8206	0.7335	0.7030	0.8774	0.9673	0.9050
	CG_5	0.7710	0.4832	0.9399	0.9030	0.8469	0.8498	0.7997
	IB	0.4625	0.7158	0.7123	0.8114	0.6865	0.4995	0.8526
	OB	0.5795	0.4456	0.3158	0.3684	0.4413	0.3769	0.9537
	BR	0.5979	0.6983	0.8038	1.0252	0.7729	0.8329	0.8822
5–6	CG_1	0.8022	0.4289	0.3979	1.0552	0.7667	0.7204	0.8657
	CG_2	0.6202	0.9708	0.8567	1.4238	1.1128	0.8677	0.8500
	CG_3	0.6936	0.8658	0.6440	0.6689	0.9594	0.9227	0.9094
	CG_4	0.8055	0.6127	0.6613	0.7786	0.6073	0.8448	0.8786
	CG_5	0.7937	0.7917	0.9494	0.5881	1.0359	0.8378	0.7574
	IB	0.7181	0.7856	0.6351	0.9424	0.8566	0.5830	0.8379
	OB	0.2965	0.7180	0.8312	0.4867	0.4148	0.3906	0.8918
	BR	0.5457	0.9838	0.4932	1.3509	0.6377	0.9034	0.7874
7–8	CG_1	N.A	N.A	N.A	N.A.	N.A	N.A.	N.A.
	CG_2	0.8155	0.8659	0.4836	1.0012	1.2820	0.9324	0.8821
	CG_3	0.9068	0.8202	0.9517	0.7985	0.9208	0.8498	0.7828
	CG_4	0.8744	0.7812	0.7397	0.5944	1.0338	0.9576	0.8317
	CG_5	0.6707	0.6716	0.5436	0.7258	0.7382	0.7351	0.7931
	IB	0.8850	0.6881	0.4820	0.6317	0.8182	0.5572	0.8978
	OB	0.8078	0.5351	0.5359	0.9247	0.8215	0.5687	0.8980
	BR	0.8975	0.9474	0.6670	1.2224	0.8760	0.5867	0.9982
9–10	CG_1	N.A	N.A	N.A	N.A.	N.A	N.A.	N.A.
	CG_2	0.8973	0.7892	0.5995	1.0770	0.8751	0.9516	0.8045
	CG_3	0.8796	0.9599	0.5261	0.8689	0.8289	0.8291	0.9857
	CG_4	0.8672	0.8836	0.9331	0.7205	0.7450	0.8242	0.8116
	CG_5	0.9456	0.9272	0.8451	1.0275	0.8351	0.8946	0.8886
	IB	0.5929	0.6924	0.5735	0.7493	1.0680	0.6811	0.8702
	OB	0.6660	0.6639	0.4459	0.9431	0.6141	0.6692	0.8429
	BR	0.5716	0.5592	0.9274	1.2150	1.2985	0.5727	0.9093
11–12	CG_1	N.A	N.A	N.A	N.A.	N.A	N.A.	N.A.
	CG_2	0.7280	0.8680	0.9869	1.0243	1.2205	0.9528	0.9281
	CG_3	0.8577	0.7717	0.6415	0.8895	1.0290	1.0113	0.8092
	CG_4	0.7816	0.6070	0.7155	0.8524	1.1664	0.6964	0.8307
	CG_5	0.8952	0.7062	0.6234	1.2040	1.2776	0.7392	0.7796
	IB	0.6429	0.8082	0.5423	1.0245	0.9105	0.6996	0.7302
	OB	0.5985	0.7263	0.4530	0.8633	0.7611	0.6456	0.8442
	BR	0.6102	0.5571	0.5861	9.9702	0.8232	0.6799	0.9878
13–14	CG_1	N.A	N.A	N.A	N.A.	N.A	N.A.	N.A.
	CG_2	0.9131	0.9483	0.7897	0.5951	1.2302	0.8678	0.8855
	CG_3	0.8640	0.9436	0.7995	0.8448	1.3351	0.8413	0.9020
	CG_4	0.8440	0.8317	0.7884	0.7632	0.8955	0.6835	0.8361

(*continued on next page*)

Table 8 (*continued*)

Stories	Groups	GSS	MCC-EB	UEBB-BC	QDSO	VPS-MBLSIII	PHSMJA	CCS
	CG_5	0.7504	0.5183	0.6543	0.9678	1.2381	0.5646	0.8171
	IB	0.4334	0.7649	0.5768	0.7235	1.0583	0.7407	0.8017
	OB	0.5838	0.8759	0.5930	0.7234	0.6629	0.6376	0.9335
	BR	0.5739	0.9633	0.4671	8.9442	1.2950	0.4742	0.9346
15–16	CG_1	N.A	N.A	N.A	N.A.	N.A	N.A.	N.A.
	CG_2	0.7900	0.7095	0.7252	0.8329	0.5999	0.7012	0.8247
	CG_3	0.6169	0.8363	0.5253	1.0164	0.8000	0.8035	0.8333
	CG_4	0.8925	0.7092	0.4719	0.9299	0.6660	0.7880	0.8289
	CG_5	0.7392	0.2343	0.3991	0.7129	0.8518	0.7154	0.8644
	IB	0.4174	0.9043	0.5068	0.6965	1.0137	0.5809	0.8860
	OB	0.9349	0.8286	0.4202	0.6753	0.6695	0.6878	0.8442
	BR	0.8143	0.8690	0.8913	8.2226	1.1942	0.4903	0.8188
17–18	CG_1	N.A	N.A	N.A	N.A.	N.A	N.A.	N.A.
	CG_2	0.6376	0.8179	0.5091	0.8787	0.9209	0.5863	0.7769
	CG_3	0.6305	0.8377	0.5442	0.8509	0.5038	0.8908	0.9581
	CG_4	0.7874	0.5820	0.5459	0.9143	0.6384	0.9257	0.7634
	CG_5	0.8161	0.3428	0.4074	0.8291	0.4976	0.4692	0.9405
	IB	0.6746	0.7062	0.4471	0.7560	0.8547	0.6104	0.9299
	OB	0.6940	0.7033	0.3754	0.3746	0.7985	0.6898	0.7756
	BR	0.8602	0.8820	0.6507	1.1395	0.9106	0.4434	0.9664
19–20	CG_1	N.A	N.A	N.A	N.A.	N.A	N.A.	N.A.
	CG_2	0.8505	0.6175	0.4676	0.5807	0.6258	0.7041	0.6640
	CG_3	0.8909	0.7875	0.5559	0.5982	0.7242	0.5986	0.7938
	CG_4	0.5532	0.4686	0.3903	0.5080	0.4574	0.5012	0.8751
	CG_5	0.3815	0.2082	0.4388	0.4772	0.3456	0.3160	0.8368
	IB	0.5365	0.6416	0.5260	0.6309	0.6382	0.5177	0.9179
	OB	0.4109	0.3554	0.4043	0.5299	0.6878	0.6886	0.8151
	BR	0.9735	0.2187	0.7315	3.9712	1.0539	0.7957	1.0000
Max. DCR		0.9735	0.9838	0.9959	9.9702	1.3351	1.0113	1.0000
Min. DCR		0.2965	0.2082	0.3158	0.2535	0.3456	0.3094	0.6640
Mean DCR		0.7247	0.7133	0.6274	1.2210	0.8475	0.7071	0.8600
Standard deviation		0.1607	0.2007	0.1765	1.6837	0.2489	0.1744	0.0716
Max. IDR		0.8566	0.9714	0.6613	1.1122	1.2074	0.8934	0.9936
Max. Roof displacement		0.5930	0.6533	0.4436	0.8172	0.8786	0.5786	0.7939
Geometric const. considered?		NO	NO	NO	NO	NO	YES	YES
Geometric constraints violated?		YES	YES	YES	YES	YES	NO	NO

solutions of the QDSO, Tribe-ISA methods, yet those designs are infeasible because they violate the strength constraints. A design check and verification process performed by the authors indicate that although considered, the geometric constraints are violated in the reported optimum solution of the PHSMJA method, and no such constraint violations exist in the solution produced with the proposed CCS algorithm in this study.

4.4. Design example 3: 3860-member steel frame

The third design example is a 20-story and 3860-member steel frame (Fig. 5) consisting of 1064 columns, 1836 beams, and 960 bracings. The stability of the frame is established using moment-resisting connections as well as X-type bracing systems along the *x* and *y* directions. The beam elements are continuously braced along their lengths by the floor system; while the columns and bracings are assumed to be unbraced along their lengths. The effective length factor, *K*, is taken as one for buckling of the columns, beams, and bracings. For practical fabrication requirements, the 3860 members of the frame are grouped into 73 independent discrete sizing variables. The member grouping is performed both at the plan and elevation levels. At the plan level, the columns are collected under five different groups (CG_1 to CG_5) as shown in Fig. 5h; the beams are collected under two groups as inner and outer beams; and all the bracings are assigned to a single group. At the elevation level, the structural members are required to have the same sections in every two stories, resulting in 43 column groups, 20 beam groups, and 10 bracing groups for the frame.

A comparison of the optimum design of the CCS technique with the previously reported solutions of this frame in the literature is presented in Table 7. It can be seen from this table that the CCS outperforms all other methods in terms of the quality of the optimum design achieved, and it ranks second in terms of speed of convergence to the optimum solution. In fact, the CCS produces the best-known solution of this design example in the literature, resulting in an optimum design weight of 2353.65 tons for the frame by implementing 997 structural analyses only. The solutions of the other methods are 3539.83 tons obtained with 900 analyses by GSS; 2972.64 tons obtained with 50,000 analyses by MCC-MB; 4117.43 tons obtained with 9979 analyses by UEBB-BC; 2703.32 tons obtained with 17,000 analyses by QDSO; 2787.50 tons obtained with 20,000 analyses by VPS-MBLSIII; and 3013.10 tons obtained with 48,622 analyses by PHSMJA. A statistical treatment of the fifteen independent runs performed with the CCS reveals that the algorithm produces a mean design weight of 2446.31 tons with a standard deviation of 78.89 and a coefficient of variation of 0.03, indicating its robustness and reliability.

In Table 8, the feasibility of the optimum designs produced to this design example by the CCS algorithm and other methods is investigated in terms of related strength and displacement constraints. It can be seen from this table that amongst the reported solutions of the problem, those produced by the GSS, MCC-MB, UEBB-BC, and CCS methods satisfactorily meet all of the strength and displacement requirements, whereas those produced by QDSO, VPS-MBLSIII and PHSMJA methods fail to satisfy strength and displacement requirements at least for one design group. It is also

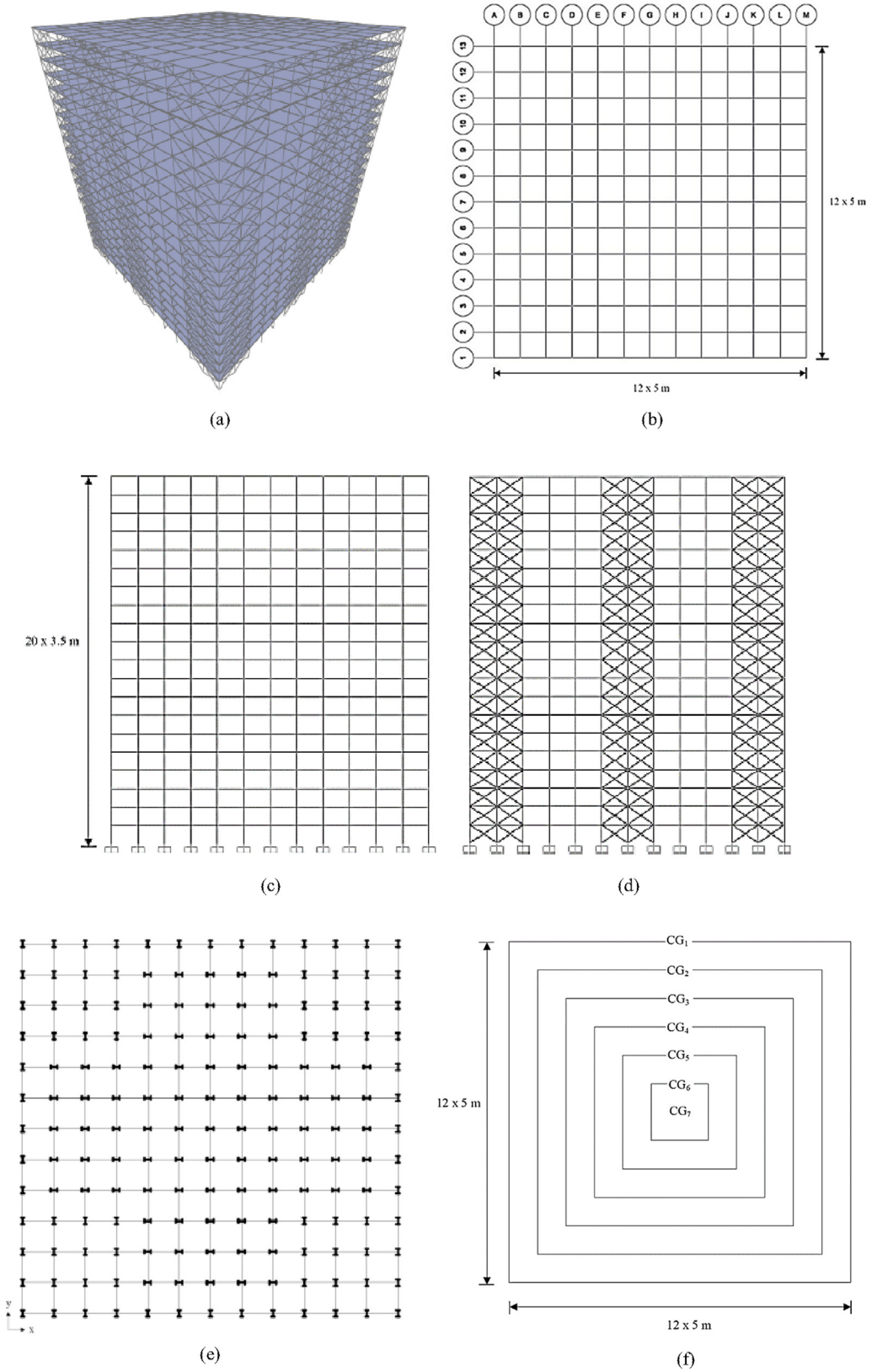

Fig. 6. 11540-member steel frame. (a) 3-D view, (b) plan view, (c) side view of the frames 2, 3, 4, 6, 7, 8, 10, 11, 12, B, C, D, F, G, H, J, K and L, (d) side view of the frames 1, 5, 9, 13, A, E, I and M, (e) orientation of the columns (f) grouping of the columns (Kazemzadeh Azad and Hasançebi, 2015).

important to note that as compared to the other feasible solutions of the problem, the CCS algorithm yields an optimum design having the highest mean (0.8600) and the lowest standard deviation (0.0716) for DCR values of the member groups, indicating that a more uniform and efficient overall strength demand distribution is achieved for the frame with the proposed CCS algorithm.

Table 8 also analyzes whether the geometric constraints have been considered while solving the problem by different methods,

Table 9
The optimum designs reported for the 11540-member steel frame with various methods.

Stories	Groups	UEBB-BC	GSS	CCS	Stories	Groups	UEBB-BC	GSS	CCS
1–2	CG_1	W40X431	W36X393	W36X439	11–12	CG_1	W14X176	W24X408	W30X261
	CG_2	W33X291	W40X249	W27X217		CG_2	W12X106	W33X118	W12X190
	CG_3	W36X300	W36X393	W12X336		CG_3	W30X235	W18X234	W27X161
	CG_4	W12X190	W40X297	W40X235		CG_4	W40X431	W36X328	W40X174
	CG_5	W36X393	W44X335	W14X398		CG_5	W36X256	W30X235	W36X194
	CG_6	W12X279	W18X258	W18X234		CG_6	W33X221	W36X170	W36X170
	CG_7	W40X264	W40X431	W40X211		CG_7	W36X170	W27X146	W24X117
	IB	W18X35	W18X40	W12X19		IB	W40X183	W40X199	W30X124
	OB	W27X146	W21X57	W8X24		OB	W8X28	W33X291	W18X234
	BR	W18X130	W18X211	W14X99		BR	W30X124	W21X62	W21X62
3–4	CG_1	W30X477	W24X250	W30X292	13–14	CG_1	W27X307	W24X250	W36X245
	CG_2	W40X199	W40X372	W30X191		CG_2	W24X131	W33X118	W40X174
	CG_3	W30X261	W44X262	W30X235		CG_3	W33X118	W30X191	W14X120
	CG_4	W40X174	W36X256	W12X210		CG_4	W33X118	W40X264	W30X132
	CG_5	W33X263	W40X277	W44X262		CG_5	W36X170	W21X93	W24X146
	CG_6	W27X178	W27X258	W24X207		CG_6	W36X280	W33X241	W30X132
	CG_7	W12X190	W33X291	W14X211		CG_7	W21X132	W16X89	W24X94
	IB	W24X84	W16X26	W18X35		IB	W24X55	W27X84	W21X93
	OB	W36X182	W18X40	W18X40		OB	W27X235	W33X291	W27X178
	BR	W30X211	W33X130	W10X100		BR	W21X62	W27X129	W21X62
5–6	CG_1	W24X335	W44X290	W33X263	15–16	CG_1	W30X211	W24X117	W24X207
	CG_2	W40X211	W18X234	W40X183		CG_2	W14X68	W24X84	W24X103
	CG_3	W18X283	W44X335	W36X232		CG_3	W12X96	W36X256	W10X100
	CG_4	W27X307	W36X245	W12X252		CG_4	W14X159	W36X232	W30X116
	CG_5	W36X280	W33X241	W36X256		CG_5	W14X74	W16X89	W33X118
	CG_6	W40X199	W18X258	W12X210		CG_6	W14X74	W33X130	W30X90
	CG_7	W36X170	W44X290	W30X191		CG_7	W12X58	W40X167	W18X76
	IB	W40X235	W40X174	W30X132		IB	W18X35	W24X62	W21X83
	OB	W12X26	W40X199	W36X160		OB	W16X36	W18X60	W36X182
	BR	W12X72	W27X94	W14X68		BR	W14X61	W21X68	W12X40
7–8	CG_1	W36X359	W21X182	W36X260	17–18	CG_1	W33X318	W18X192	W24X117
	CG_2	W24X117	W33X152	W14X193		CG_2	W12X96	W24X117	W24X76
	CG_3	W44X262	W18X175	W27X217		CG_3	W40X167	W33X118	W8X67
	CG_4	W40X215	W33X291	W27X235		CG_4	W30X90	W44X262	W14X68
	CG_5	W14X283	W27X178	W27X235		CG_5	W21X62	W44X335	W18X71
	CG_6	W27X194	W40X199	W40X199		CG_6	W18X65	W40X297	W21X68
	CG_7	W30X173	W24X250	W18X192		CG_7	W14X48	W36X160	W18X55
	IB	W10X22	W36X135	W27X114		IB	W14X22	W36X150	W24X55
	OB	W36X280	W24X68	W24X146		OB	W40X321	W24X62	W18X76
	BR	W36X135	W40X174	W12X58		BR	W12X58	W21X62	W8X40
9–10	CG_1	W40X297	W40X372	W36X280	19–20	CG1	W30X132	W18X119	W12X152
	CG_2	W36X135	W33X169	W21X182		CG2	W27X102	W33X152	W12X30
	CG_3	W12X152	W24X250	W18X192		CG3	W24X131	W24X76	W14X34
	CG_4	W33X291	W30X261	W24X207		CG4	W30X124	W16X36	W8X28
	CG_5	W30X191	W24X335	W12X230		CG5	W12X53	W16X36	W10X39
	CG_6	W36X280	W27X178	W33X169		CG6	W8X28	W18X143	W12X30
	CG_7	W18X119	W27X448	W24X131		CG7	W6X15	W30X108	W12X30
	IB	W33X130	W24X55	W30X124		IB	W40X278	W24X55	W14X22
	OB	W10X30	W40X277	W30X235		OB	W12X26	W40X167	W21X68
	BR	W24X94	W27X94	W14X53		BR	W8X31	W18X40	W8X28
Best weight (ton)							10756.63	10707.53	8516.65
Structural analyses							7616	2100	996
Worst weight (ton)							–	11895.78	9782.75
Mean weight (ton)							–	11236.91	9100.38
Standard deviation							–	459.64	314.41
Coefficient of variation							–	0.04	0.03

and whether any geometric constraint violation is detected in the reported optimum solutions. It is noted that the geometric constraints are not considered and imposed while solving the problem with GSS, MCC-MB, UEBB-BC, QDSO, and VPS-MBLSIII methods. Hence, those constraints, as anticipated, are not satisfied in the reported optimum solutions of the problem with these methods. The geometric constraints are satisfied in the optimum solution of the PHSMJA method, yet this solution is infeasible because it violates the strength constraints. A design check and verification process performed by the authors indicates no constraint violation for the optimum solution produced with the proposed CCS algorithm in this study.

4.5. Design example 4: 11540-member steel frame

The last design example is a 20-story and 11540-member steel frame (Fig. 6) consisting of 3380 columns, 6240 beams, and 1920 bracings. The stability of the frame is established using moment-resisting connections as well as X-type bracing systems along the $\times$ and y directions. The beam elements are all continuously braced along their lengths by the floor system while the columns and bracings are assumed to be unbraced along their lengths. The effective length factor, K, is taken as 1.0 for buckling of columns, beams, and bracings. For practical fabrication requirements, the 11,540 members of the frame are grouped into 100 indepen-

Table 10
DCRs and maximum displacement constraint ratios in the reported optimum designs of the 11540-member steel frame.

Stories	Groups	UEBB-BC	GSS	CCS	Stories	Groups	UEBB-BC	GSS	CCS
1–2	CG_1	0.9225	0.9850	0.9880	11–12	CG_1	0.6746	0.8059	0.7782
	CG_2	0.7365	0.6279	0.8195		CG_2	0.9014	0.8486	0.7146
	CG_3	0.8299	0.9796	0.9565		CG_3	0.7142	0.7790	0.8433
	CG_4	0.7093	0.9753	0.9270		CG_4	0.6100	0.6049	0.8681
	CG_5	0.9956	0.9657	0.9111		CG_5	0.7959	0.7595	0.8944
	CG_6	0.7899	0.6933	0.8678		CG_6	0.8172	0.7188	0.7715
	CG_7	0.5621	0.7714	0.9854		CG_7	0.8684	0.7005	0.8398
	IB	0.4945	0.5586	0.9281		IB	0.5832	0.7760	0.8299
	OB	0.4671	0.5054	0.9328		OB	0.6988	0.9118	0.7292
	BR	0.5870	0.6607	0.7143		BR	0.9081	0.5329	0.9803
3–4	CG_1	0.9924	0.6432	0.9405	13–14	CG_1	0.8820	0.7664	0.8020
	CG_2	0.4712	0.7436	0.8162		CG_2	0.7948	0.8774	0.8297
	CG_3	0.8503	0.7964	0.9338		CG_3	0.6635	0.9771	0.8103
	CG_4	0.7877	0.9711	0.8486		CG_4	0.5628	0.9296	0.8365
	CG_5	0.8398	0.9195	0.9660		CG_5	0.9938	0.8626	0.8076
	CG_6	0.6855	0.9773	0.8639		CG_6	0.5733	0.5365	0.8020
	CG_7	0.7544	0.8942	0.7833		CG_7	0.8218	0.6380	0.9341
	IB	0.7450	0.7004	0.8064		IB	0.6538	0.8642	0.7263
	OB	0.7329	0.7042	0.8024		OB	0.6197	0.9063	0.9525
	BR	0.8406	0.4606	0.9024		BR	0.4861	0.8927	0.8769
5–6	CG_1	0.8808	0.8324	0.9542	15–16	CG_1	0.9681	0.6983	0.9936
	CG_2	0.7647	0.9219	0.9148		CG_2	0.7479	0.7973	0.7947
	CG_3	0.6664	0.8271	0.8134		CG_3	0.3741	0.7358	0.7756
	CG_4	0.8368	0.7334	0.7551		CG_4	0.5104	0.5564	0.7660
	CG_5	0.9018	0.9773	0.8430		CG_5	0.7458	0.8778	0.7872
	CG_6	0.7358	0.9909	0.8063		CG_6	0.5883	0.9227	0.8628
	CG_7	0.6839	0.9259	0.7755		CG_7	0.3978	0.8846	0.7983
	IB	0.7761	0.7130	0.7732		IB	0.6712	0.7811	0.7955
	OB	0.8546	0.8148	0.9813		OB	0.7559	0.9304	0.9068
	BR	0.7872	0.5905	0.8807		BR	0.9301	0.7478	0.8954
7–8	CG_1	0.9290	0.9366	0.9181	17–18	CG_1	0.5242	0.9085	0.9508
	CG_2	0.9871	0.9583	0.7854		CG_2	0.4698	0.3690	0.8012
	CG_3	0.9372	0.7784	0.8016		CG_3	0.6762	0.4360	0.7790
	CG_4	0.7191	0.8626	0.8042		CG_4	0.5097	0.5739	0.8049
	CG_5	0.9793	0.7133	0.8637		CG_5	0.5273	0.9006	0.9071
	CG_6	0.8897	0.7941	0.8804		CG_6	0.3327	0.8314	0.8269
	CG_7	0.6936	0.6795	0.6933		CG_7	0.2927	0.7155	0.9008
	IB	0.6654	0.9624	0.8116		IB	0.6218	0.9916	0.7265
	OB	0.8476	0.9955	0.9148		OB	0.7177	0.8301	0.8547
	BR	0.4346	0.7594	0.7661		BR	0.5474	0.5933	0.8121
9–10	CG_1	0.8396	0.8442	0.8779	19–20	CG1	0.7240	0.8000	0.5846
	CG_2	0.7205	0.9968	0.7909		CG2	0.4059	0.7935	0.9685
	CG_3	0.6846	0.9334	0.7909		CG3	0.4519	0.7793	0.8727
	CG_4	0.6566	0.6745	0.8013		CG4	0.7628	0.7342	0.8699
	CG_5	0.5392	0.8948	0.8047		CG5	0.7293	0.9851	0.6645
	CG_6	0.7380	0.6533	0.8556		CG6	0.2640	0.9531	0.8964
	CG_7	0.3668	0.8256	0.8985		CG7	0.2899	0.8241	0.8011
	IB	0.7739	0.7587	0.7730		IB	0.4787	0.3635	0.9765
	OB	0.8693	0.8482	0.9228		OB	0.4713	0.7906	0.7697
	BR	0.7558	0.9508	0.9648		BR	0.9439	0.8325	0.9955
Max. DCR							0.9956	0.9968	0.9955
Min. DCR							0.2640	0.3635	0.5846
Mean DCR							0.6976	0.7931	0.8468
Standard deviation							0.1778	0.1475	0.0804
Max. IDR							0.6537	0.7957	0.8325
Max. Roof displacement							0.4941	0.5477	0.6552
Geometric constraints considered?							NO	NO	YES
Geometric constraints violated?							YES	YES	NO

dent discrete sizing variables. The member grouping is performed both at the plan and elevation levels. At the plan level, columns are collected under seven different groups (CG_1 to CG_7) as shown in Fig. 6f; the beams are collected under two groups as inner and outer beams; and all the bracings are assigned to a single group. At the elevation level, the structural members are required to have the same sections in every two stories, resulting in 70 column groups, 20 beam groups, and 10 bracing groups for the frame.

A comparison of the optimum design of the CCS technique with the previously reported solutions of this frame in the literature is presented in Table 9. It can be seen from this table that the CCS outperforms all other methods in terms of both the quality of the optimum design and speed of convergence to the optimum solution. In fact, the CCS produces the best-known solution of this design example in the literature, resulting in an optimum design weight of 8516.65 tons for the frame by implementing 996 structural analyses only. The solutions of the other methods are 10756.63 tons obtained with 7616 analyses by UEBB-BC and 10707.53 tons obtained with 2100 analyses by GSS. A statistical treatment of the fifteen independent runs performed with the

CCS reveals that the algorithm produces a mean design weight of 9100.38 tons with a standard deviation of 314.41 and a coefficient of variation of 0.03, indicating its robustness and reliability.

In Table 10, the feasibility of the optimum designs produced to this design example by the CCS algorithm and other methods is investigated in terms of related strength and displacement constraints. It can be seen from this table that the solutions reported by all the methods satisfy all the strength and displacement requirements. It is also important to note that as compared to the other solutions of the problem, the CCS algorithm yields an optimum design having the highest mean (0.8468) and the lowest standard deviation (0.0804) for DCR values of the member groups, indicating that a more uniform and efficient overall strength demand distribution is achieved for the frame with the proposed CCS algorithm.

Table 10 also analyzes whether the geometric constraints have been considered while solving the problem by different methods, and whether any geometric constraint violation is detected in the reported optimum solutions. It is noted that the geometric constraints are not considered and imposed while solving the problem with UEBB-BC and GSS methods. Hence, those constraints, as anticipated, are not satisfied in the reported optimum solutions of the problem with these methods. A design check and verification process performed by the authors indicates no constraint violation for the optimum solution produced with the proposed CCS algorithm in this study.

5. Concluding remarks

In this paper, a novel design-driven structural optimization algorithm called the capacity control search (CCS) method is proposed for discrete sizing optimization of steel frames. The CCS algorithm encourages an explorative search in the early stages of the optimization, and as the iterations continue, an exploitative search is facilitated by the algorithm under the guidance of the maximum demand to capacity ratios (DCRs) calculated for member groups. The performance of the CCS algorithm has been investigated numerically using four steel frame examples, in which the optimum designs attained with the CCS algorithm are compared with the previously published solutions of these problems in the literature. For each problem considered, a design check and verification process are also performed by the authors not only for the solution produced with the CCS algorithm but also for all other solutions of the problem in the literature to investigate the feasibility of the optimum solutions reported for a sound comparison between different methods. It has been noted that the CCS algorithm produces the best-known solutions of these design examples in the literature until now, converging to optimum designs by performing less than a thousand structural analyses. Besides, a statistical treatment of the independent runs performed with the CCS verifies the robustness and reliability of the algorithm.

Data availability

Data will be made available on request.

Declaration of Competing Interest

The authors declare that they have no known competing financial interests or personal relationships that could have appeared to influence the work reported in this paper.

References

[1] Saka MP, Hasançebi O, Geem ZW. Metaheuristics in structural optimization and discussions on harmony search algorithm. Swarm Evol Comput 2016;28:88–97. https://doi.org/10.1016/j.swevo.2016.01.005.

[2] Gholizadeh S, Danesh M, Gheyratmand C. A new Newton metaheuristic algorithm for discrete performance-based design optimization of steel moment frames. Comput Struct 2020;234:. https://doi.org/10.1016/j.compstruc.2020.106250106250.

[3] Sarma KC, Adeli H. Bilevel parallel genetic algorithms for optimization of large steel structures. Comput-Aided Civ Infrastruct Eng 2001;16(5):295–304. https://doi.org/10.1111/0885-9507.00234.

[4] Papadrakakis M, Lagaros ND, Fragakis Y. Parallel computational strategies for structural optimization. Int J Numer Meth Eng 2003;58(9):1347–80. https://doi.org/10.1002/nme.821.

[5] Hasançebi O, Bahçecioğlu T, Kurç Ö, Saka MP. Optimum design of high-rise steel buildings using an evolution strategy integrated parallel algorithm. Comput Struct 2011;89(21–22):2037–51. https://doi.org/10.1016/j.compstruc.2011.05.019.

[6] Kaveh A, Gholipour Y, Rahami H. Optimal design of transmission towers using genetic algorithm and neural networks. Int J Space Struct 2008;23(1):1–19. https://doi.org/10.1260/026635108785342073.

[7] Gholizadeh S. Performance-based optimum seismic design of steel structures by a modified firefly algorithm and a new neural network. Adv Eng Softw 2015;81(C):50–65. https://doi.org/10.1016/j.advengsoft.2014.11.003.

[8] Gholizadeh S, Milany A. Optimal performance-based design of steel frames using advanced metaheuristics. Asian J Civil Eng 2016;17(5):607–23.

[9] Papadrakakis M, Lagaros ND, Tsompanakis Y. Structural optimization using evolution strategies and neural networks. Comput Methods Appl Mech Eng 1998;156(1–4):309–33. https://doi.org/10.1016/S0045-7825(97)00215-6.

[10] Kaveh A, Laknejadi K, Alinejad B. Performance-based multi-objective optimization of large steel structures. Acta Mech 2012;223(2):355–69. https://doi.org/10.1007/s00707-011-0564-1.

[11] Ting TO, Yang XS, Cheng S, Huang K. Hybrid metaheuristic algorithms: Past, present, and future. Stud Comput Intelligence 2015;585(January):71–83. https://doi.org/10.1007/978-3-319-13826-8_4.

[12] Kaveh A, Talatahari S. A hybrid CSS and PSO algorithm for optimal design of structures. Struct Eng Mech 2012;42(6):783–97. , https://doi.org/10.12989/sem.2012.42.6.783.

[13] Kaveh A, Bakhshpoori T, Afshari E. An efficient hybrid particle swarm and swallow swarm optimization algorithm. Comput Struct 2014;143:40–59. https://doi.org/10.1016/j.compstruc.2014.07.012.

[14] Kaveh A, Mahdavi VR. A hybrid CBO-PSO algorithm for optimal design of truss structures with dynamic constraints. Appl Soft Comput J 2015;34:260–73. https://doi.org/10.1016/j.asoc.2015.05.010.

[15] Cheng MY, Prayogo D, Wu YW, Lukito MM. A hybrid harmony search algorithm for discrete sizing optimization of truss structure. Autom Constr 2016;69:21–33. https://doi.org/10.1016/j.autcon.2016.05.023.

[16] Kaveh A, Ilchi GM. A new hybrid meta-heuristic algorithm for optimal design of large-scale dome structures. Eng Optim 2018;50(2):235–52. https://doi.org/10.1080/0305215X.2017.1313250.

[17] Dillen W, Lombaert G, Schevenels M. A hybrid gradient-based/metaheuristic method for Eurocode-compliant size, shape and topology optimization of steel structures. Eng Struct 2021;239:. https://doi.org/10.1016/j.engstruct.2021.112137112137.

[18] Tayfur B, Yilmaz H, Daloğlu AT. Hybrid tabu search algorithm for weight optimization of planar steel frames. Eng Optim 2021;53(8):1369–83. https://doi.org/10.1080/0305215X.2020.1793977.

[19] Kazemzadeh AS. Enhanced hybrid metaheuristic algorithms for optimal sizing of steel truss structures with numerous discrete variables. Struct Multidiscip Optim 2017;55(6):2159–80. https://doi.org/10.1007/s00158-016-1634-8.

[20] Patnaik SN, Gendy AS, Berke L, Hopkins DA. Modified fully utilized design (MFUD) method for stress and displacement constraints. Int J Numer Meth Eng 1998;41(7):1171–94. https://doi.org/10.1002/(SICI)1097-0207(19980415)41:7%3C1171::AID-NME296%3E3.0.CO;2-O.

[21] Ahrari A, Atai AA. Fully stressed design evolution strategy for shape and size optimization of truss structures. Comput Struct 2013;123:58–67. https://doi.org/10.1016/j.compstruc.2013.04.013.

[22] Ahrari A, Deb K. An improved fully stressed design evolution strategy for layout optimization of truss structures. Comput Struct 2016;164:127–44. https://doi.org/10.1016/j.compstruc.2015.11.009.

[23] Flager F, Soremekun G, Adya A, Shea K, Haymaker J, Fischer M. Fully constrained design: a general and scalable method for discrete member sizing optimization of steel truss structures. Comput Struct 2014;140:55–65. https://doi.org/10.1016/j.compstruc.2014.05.002.

[24] Park HS, Park CL. Drift control of high-rise buildings with unit load method. Struct Design Tall Build 1997;6(1):23–35. https://doi.org/10.1002/(SICI)1099-1794(199703)6:1%3C23::AID-TAL80%3E3.0.CO;2-1.

[25] Chan CM. Optimal lateral stiffness design of tall buildings of mixed steel and concrete construction. Struct Des Tall Build 2001;10(3):155–77. https://doi.org/10.1002/tal.170.

[26] Elvin A, Walls R, Cromberge D. Optimising structures using the principle of virtual work. J South African Inst Civil Eng 2009;51(2):11–9. , https://hdl.handle.net/10520/EJC27035.

[27] Walls R, Elvin A. Optimizing structures subject to multiple deflection constraints and load cases using the principle of virtual work. J Struct Eng 2010;136(11):1444–52. https://doi.org/10.1061/(ASCE)ST.1943-541X.0000246.
[28] Kazemzadeh Azad S, Hasançebi O, Saka MP. Guided stochastic search technique for discrete sizing optimization of steel trusses: A design-driven heuristic approach. Comput Struct 2014;134:62–74. https://doi.org/10.1016/j.compstruc.2014.01.005.
[29] Kazemzadeh Azad S, Hasançebi O. Computationally efficient discrete sizing of steel frames via guided stochastic search heuristic. Comput Struct 2015;156:12–28. https://doi.org/10.1016/j.compstruc.2015.04.009.
[30] American Institute of Steel Construction (AISC). Manual of steel construction, load and resistance factor design (LRFD). 2nd ed. Chicago; 1994.
[31] ASCE 7-98. Minimum design loads for buildings and other structures: revision of ANSI/ASCE 7-95. American Society of Civil Engineers; 2000.
[32] Kazemzadeh AS. Design optimization of real-size steel frames using monitored convergence curve. Struct Multidiscip Optim 2021;63(1):267–88. https://doi.org/10.1007/s00158-020-02692-3.
[33] Hasançebi O, Erdal F, Saka MP. Adaptive harmony search method for structural optimization. J Struct Eng 2010;136(4):419–31. https://doi.org/10.1061/(ASCE)ST.1943-541X.0000128.
[34] Kazemzadeh Azad S, Hasançebi O, Kazemzadeh AS. Upper bound strategy for metaheuristic-based design optimization of steel frames. Adv Eng Softw 2013;57:19–32. https://doi.org/10.1016/j.advengsoft.2012.11.016.
[35] Kazemzadeh Azad S, Hasançebi O, Kazemzadeh AS. Computationally efficient optimum design of large-scale steel frames. Int J Optimization Civil Eng 2014;4(2):233–59.
[36] Talatahari S, Azizi M. Optimal design of real-size building structures using quantum-behaved developed swarm optimizer. Struct Des Tall Special Build 2020;29:e1747.
[37] Talatahari S, Azizi M. Optimum design of building structures using tribe-interior search algorithm. Structures 2020;28:1616–33. https://doi.org/10.1016/j.istruc.2020.09.075.
[38] Talatahari S, Jalili S, Azizi M. Optimum design of steel building structures using migration-based vibrating particles system. Structures 2021;33:1394–413. https://doi.org/10.1016/j.istruc.2021.05.028.
[39] Kaveh A, Khodadadi N, Talatahari S. Comparative study for the optimal design of steel structures using CSS and ACSS algorithms. Int J Optimization Civil Eng 2021;11(1):31–54.
[40] Uğur IB. Optimum design of large-scale steel structures using metaheuristic optimization. Dicle University; 2021. PhD Thesis..